# Food & Function



**PAPER** 

View Article Online
View Journal | View Issue



**Cite this:** Food Funct., 2024, **15**, 12146

# Deciphering the potential of *Cymbopogon citratus* (DC.) Stapf as an anti-obesity agent: phytochemical profiling, *in vivo* evaluations and molecular docking studies†

Omnia Aly, ‡<sup>a</sup> Reham Hassan Mekky, (1) ‡<sup>b</sup> Florbela Pereira, (1) ‡<sup>c</sup> Yasser M. Diab, d Mohamed A. Tammam (1) \*<sup>d</sup> and Amr El-Demerdash (1) \*<sup>e,f</sup>

Based on its anti-inflammatory and antioxidant properties, Cymbopogon citratus (DC) Stapf is commonly used in traditional and modern medicine to cure different diseases. The present study investigates the potential of C. citratus organic extract as an anti-obesity drug in a HCHFD (high-carbohydrate, high-fat diet) model for obese rats. Its negative hypolipidemic effect has been confirmed through biochemical and histological methods. Fifty male albino rats were randomly divided into five groups (10 rats each) Group I (Control group), Group II (HCHFD group), Group III (C. citratus group), Group IV (HCHFD + C. citratus group) and Group V (HCHFD + Orlistat group). Serum glucose levels and lipid profiles were quantified using a spectrophotometer. Insulin, apelin, and adiponectin parameters were measured using ELISA (enzyme-linked immunosorbent assay) kits, while real-time PCR following extraction and purification was used for apelin, apelin receptor genes (APJ), and adiponectin gene expression evaluation. Besides, C. citratus methanolic extract was subjected to untargeted metabolic profiling via RP-HPLC-QTOF-MS and MS/MS, disclosing the presence of 52 secondary metabolites where they mainly belonged to phenolic compounds viz., flavones and hydroxycinnamic acids, among other metabolites with predominance of derivatives of luteolin and O-coumaroyl-O-feruloylglycerol. Our findings were further strengthened by computational-based virtual screening protocols that included molecular docking (MDock) and Structure-Activity Relationships (SARs). The MDock studies revealed that the three main flavone-containing metabolites, each with a luteolin C6-glycosylation core featuring two sugar units (16, 25, and 31), outperformed the positive control (8EH, a triazole derivative) known to bind to the APJ protein. These metabolites exhibited exceptional binding affinities, with estimated free binding energy ( $\Delta G_B$ ) values of -9 kcal mol<sup>-1</sup> or lower, likely due to potential hydrogen bond interactions with the Arg168 residue of the APJ protein. Additionally, the pharmacokinetic, physicochemical, and toxicity profiles of the 11 major metabolites from C. citratus leaf extract were assessed, revealing a profile like that of the positive control in the three selected flavone metabolites. Based on the acquired data, it can be concluded that C. citratus shows strong potential as a hypolipidemic agent and could play a significant role in managing obesity and mitigating its associated complications.

Received 21st September 2024, Accepted 15th November 2024 DOI: 10.1039/d4fo04602a

rsc.li/food-function

E-mail: a\_eldemerdash83@mans.edu.eg,

A.Eldemerdash@uea.ac.uk; Mohamed Tammam

<sup>&</sup>lt;sup>a</sup>Department of Medical Biochemistry, National Research Centre, Cairo 12622, Egypt. E-mail: mat01@fayoum.edu.eg

<sup>&</sup>lt;sup>b</sup>Department of Pharmacognosy, Faculty of Pharmacy, Egyptian Russian University, Badr City, Cairo-Suez Road, 11829 Cairo, Egypt

<sup>&</sup>lt;sup>c</sup>LAQV REQUIMTE, Department of Chemistry, NOVA School of Science and Technology, Universidade Nova de Lisboa, 2829516 Caparica, Portugal

<sup>&</sup>lt;sup>d</sup>Department of Biochemistry, Faculty of Agriculture, Fayoum University, Fayoum 63514, Egypt

<sup>&</sup>lt;sup>e</sup>School of Chemistry, Pharmacy and Pharmacology, University of East Anglia, Norwich Research Park, Norwich NR4 7TJ, UK.

<sup>&</sup>lt;sup>f</sup>Faculty of Sciences, Mansoura University, Mansoura 35516, Egypt

<sup>†</sup> Electronic supplementary information (ESI) available. See DOI: https://doi.org/10.1039/d4fo04602a

<sup>‡</sup>These authors are equally contributed.

# 1. Introduction

On a global scale, obesity is a major and urgent public health problem, resulting in a considerable burden of disability as well as mortality. The condition of obesity is not just characterized by excessive weight. Still, it's an inflammatory systemic disease as well that is associated with diabetes, insulin resistance, cancer, heart disease, chronic renal disease, and other metabolic disorders. Adipose tissue (AT), which consists of stromal vascular cells and adipocytes, is pivotal in the development of obesity and metabolic disorders. Prolonged periods of inactivity and insufficient levels of physical exercise significantly contribute to the development of obesity and associated disorders. Within the axillary thyroid, certain adipokines, released by this endocrine gland, have a role in the development of several diseases and alter lipid and glucose metabolism significantly.<sup>1</sup>

Undoubtedly, being the largest endocrine gland, adipose tissue releases several bio-effective peptides widely referred to as adipokines. Recombinant APLN (Apelin) is a novel adipokine produced from preproapelin, consisting of 77 amino acids. By deriving a 55-amino-acid fragment from preproapelin, smaller bioactive isoforms like APLN-36, APLN-17, APLN-13, and the pyroglutamyl version of APLN-13 (Pyr-APLN-13) are generated. Smaller isoforms (Pyr) APLN-13 and -17 exhibit higher activity and are more commonly found in the bloodstream. Beyond adipose tissue, apelin and its receptor APJ are widely distributed throughout the body and synthesized in varying quantities in nearly all tissues, notably in the brain, blood vessels, heart, lung, spleen, gut, reproductive tract, and breast. Additionally, APLN and APJ play a role in other fundamental biological metabolomics pathways, including cell division, angiogenesis, cardiovascular activity, fluid balance, control of energy metabolism, consumption.2

Furthermore, over the past 25 years, since the mid-1990s, adiponectin, a 28 kDa protein adipocytokine mostly synthesized and released into the bloodstream by lean adipocytes, has been extensively researched. The principal role of adiponectin is to control the metabolism of carbohydrates and lipids. Nevertheless, the complete scope of its biological activity has yet to be clarified, encompassing a broad range of impacts on various cell and tissue categories. The protective functions of adiponectin against various disease states associated with obesity, including immunomodulatory, insulin-sensitizing, antidiabetic, anti-obesogenic, anti-inflammatory, antiatherogenic, anti-fibrotic, cardio, and neuroprotective properties, have led to its initial classification as a guardian angel adipocytokine.<sup>3</sup>

Indeed, as a substitute for traditional therapies for obesity and related issues, natural products, such as pure compounds or extracts derived from medicinal plants, are readily available in the market. These phytochemicals can elicit their antiobesity effects by various mechanisms, including the inhibition of digestive enzyme activities (pancreatic lipase and amylase), regulation of appetite, and reduction of white adipose tissue (WAT) formation or enhancement of WAT browning. Furthermore, it has been shown that the phytoconstituents present in various plants exhibit a variety of supplementary modes of action against obesity. Usually, these natural compounds restrict the development of adipose tissue by preventing the differentiation of adipocytes and adipogenesis and reducing levels of triacylglycerol by enhancing the breakdown of fats or reducing metabolic pathways involved in fat production.<sup>4</sup>

In particular, lemongrass, scientifically known as *Cymbopogon. citratus* (DC.) Stapf, is a plant extensively employed for phytoremediation because of its extraordinary resistance to certain heavy metals. The cultivated plant is largely of commercial significance to the cosmetics and perfumes sectors due to its essential oils, which consist mostly of citral. Citral is composed of two geometric isomers, geranial and neral, and has a distinctive lemon fragrance. Furthermore, *C. citratus* possesses minerals, vitamins, and bioactive substances (such as alkaloids, terpenoids, flavonoids, phenols, saponins, and tannins) that are accountable for its pharmacological characteristics (antioxidant, antifungal, anticancer, antihypertensive, antidiabetic, and anxiolytic action).<sup>5</sup>

Traditionally, the leaves of C. citratus were utilized as tea or decoction in Asia, South America, and Africa as they possessed anti-inflammatory, antiseptic, anti-dyspeptic, and anti-fever effects. They also have antispasmodic, analgesic, antipyretic, tranquillizer, anti-hermetic, diuretic, antidiabetic, and antihyperlipidemic activities. In certain regions of Asia and African countries, it has been employed to deter snakes and reptiles.<sup>6,7</sup> There traditional uses provoked several researchers to disclose the phytochemical composition and biological activities of C. citratus, in this sense, Madi et al., explored the phytochemical composition of the leaves via UPLC-Orbitrap HRMS revealing the occurrence of 21 compounds including flavonoids. The leaves also exhibited a neuroprotective effect of leaves against AlCl<sub>3</sub>-induced neurotoxicity in rats. Moreover, Costa et al., proved a strong topical anti-inflammatory ability by the carrageenan-induced rat paw edema model of the HPLC standardized organic extract of lemon grass leaves characterized by the presence of hydroxycinnamic acids and flavones. 9 Also, the leaves have a high content of essential oil with a majority of citral, among other terpenoids, where the composition of the essential oil varied according to the geographical origin, season of harvesting, extraction methods, and genetic disparities, among others.6 Besides, a plethora of studies investigated the biological potentials of the leaves, viz., antimicrobial, anti-inflammatory, antimalarial, insecticidal, antihypertensive, and anti-obesity, etc.6,7

With emphasis on the antiobesity activity of *C. citratus*, several studies focused on the antiobesity activity of lemongrass. <sup>10</sup> In this context, Da Ressurreição *et al.* <sup>11</sup> investigated the effect of *C. citratus* leaves extract, phenolic fraction, and flavonoids on the micellar solubility of cholesterol where a significant micellar destruction was noticed indicating that the intake of lemon grass could eventually disrupt various processes associated with intraluminal lipid processing, including

enzymatic hydrolysis, micelle formation, and the absorption of lipid digestion products in the colon. Moreover, Adeneye and Agbaje<sup>12</sup> investigated the effect of administration of a single, daily oral dosage of 125-500 mg kg<sup>-1</sup> of fresh leaf aqueous C. citratus extract in normal, male Wistar rats for 42 days where it caused weight loss in rats, reduced fasting plasma glucose and lipid parameters (total cholesterol), LDL-c (lowdensity lipoprotein-cholesterol), and VLD-c (Verl low-density lipoprotein cholesterol), and increased plasma HDL-c (highdensity lipoprotein-cholesterol) levels (p < 0.05) dose-dependently, without affecting plasma triglycerides. Furthermore, Kumar et al. 13 C. citratus oil's antihyperlipidaemic efficacy against dexamethasone-induced hyperlipidaemia in adult male Wistar albino rats. Treatment with C. citratus oil (100 and 200 mg kg<sup>-1</sup>, po.) significantly inhibits dexamethasone hyperlipidaemia by maintaining normal blood cholesterol, triglycerides, and atherogenic index levels.

Based on the above-mentioned data and in the context of our ongoing research program on pharmacologically active plant and marine-derived natural products, 1,14-20 we were motivated to examine the C. citratus organic extract activity as an anti-obesity agent on obese rats using adiponectin, apelin, and its receptor APJ as biomarkers for obesity as well as investigate its active constitutes using reversed-phase high-performance liquid chromatography, additionally supporting our data by a virtual screening protocol including SARs (Structure-Activity Relationships) and MDock (molecular docking). Furthermore, the pharmacokinetic profiles and physicochemical properties, as well as the toxicity profiles of the 11 major metabolites from C. citratus leaf extract (one amino acid (1), one hydroxycinnamic acid (39), eight flavones (14i, 14ii, 16, 24, 25, 31, 37, 40), and one fatty acid (48)) in our screening library were evaluated using the Deep-PK online webtool.

# Materials and methods

### 2.1. Plant material

*C. citratus* leaves were collected in the flowering stage from the Fayoum governate, Egypt. A voucher specimen of the collected sample has been settled at the plant collection of Biochemistry Department, Faculty of Agriculture, Fayoum University, Fayoum Governorate, Egypt (FAY/TP0100). The airdried leaves were extensively extracted with MeOH at room temperature, to afford after evaporation of the solvents *in vacuo* a crude extract (16.8 g).

# 2.2. *In vivo* deciphering of the anti-obesity properties of *C. citratus* extract

**2.2.1. Experimental animals.** For this study, a sample of fifty male albino rats were obtained from the animal facility of the author's institute weighting between 180 and 200 grammes at the beginning of the experiment. The rats were kept in separate, hygienic polypropylene cages and kept in a temperature-controlled chamber  $(22 \pm 2 \, ^{\circ}\text{C})$  for 12 hours of light and

12 hours of darkness each day. The objective was to create a model that accurately reflects the development of obesity in humans. The standard diet was prepared using the procedures outlined in Reeves, 1997. <sup>21</sup> In preparation for the experiment, the animals were allotted a fourteen-day interval to acclimatise to the laboratory setting. The National Research Centre's Ethics Committee in Dokki, Cairo, Egypt, approved all procedures with permission number (015420824). Additionally, the current investigation is submitted in accordance with the ARRIVE guidelines.

2.2.2. Experimental study design (experiment ran for eight weeks). A random selection of five groups, each consisting of 10 rats, was made from the obtained rats. Experimental Group I (Control group): healthy rats were allowed to be grown with standard meals. Group II (HCHFD group): the rats were provided with a diet rich in carbohydrates and fat. In Group III (C. citratus group), healthy rats were orally administered the C. citratus extract at a dosage of 125mg kg<sup>-1</sup> day<sup>-1</sup> and were allowed to be grown with standard meals. The rats in Group IV (HCHFD + C. citratus group) were administered a diet rich in carbohydrates and fat prior to receiving an oral treatment of 125 mg  $kg^{-1}$  of *C. citratus* extract for a duration of eight weeks. Group V (HCHFD + Orlistat group): rats were administered a diet rich in carbohydrates and fat followed by oral administration of orlistat at a dosage of 10 mg kg<sup>-1</sup> day<sup>-1</sup> for a duration of eight weeks.<sup>22</sup>

2.2.3. Collection of samples. Following the eight-weeks study period, the animals were fasted for eight hours before blood samples were taken. Blood was obtained from the ocular retroorbital venous plexus using capillary tubes whilst the rats were anaesthetized with formalin. The collected blood samples were then placed in clean tubes, left to coagulate, and subjected to centrifugation for 10 minutes at 3000 revolutions per minute. In order to ascertain its biochemical properties, the obtained serum was extracted and kept in a suitable container at a temperature of -20 °C. After collecting blood samples, rats were euthanized *via* cervical dislocation. The samples were stored at -80 °C for gene expression analysis. To facilitate further pathological assessment, the pancreas and liver were kept in a 10% formalin-phosphate buffered solution.

2.2.4. Biochemical analysis. The fasting blood glucose levels were measured colorimetrically, based on the protocols outlined by Passing and Bablok, 23 using commercially available enzymatic kits (BioMerieux, Marcy l'Etoile, France; Roche Diagnostics, Basel, Switzerland). To evaluate the serum insulin level, the enzyme-linked immunological sorbent assay (ELISA) developed by Yallow and Bawman was employed using a kit from BioSoure INSEASIA Co. (Nivelles, Belgium).24 The determination of insulin resistance was made using the following formula: the HOMA-IR formula, as proposed by Matthews et al., is defined as the product of fasting glucose (mg dl-1) and fasting insulin (µIU ml<sup>-1</sup>) divided by 405.<sup>25</sup> Based on the described methods by Kim et al. Cole et al. Lopes Virella et al. and Friedewald et al.,  $^{26-29}$  The serum levels of HDL (high-density lipoprotein)-cholesterol, TG (triglycerides), cholesterol, and LDL (low-density lipoprotein)cholesterol have been determined, respectively.

The levels of serum apelin (Phoenix Pharmaceuticals, Burlingame, Calif) and adiponectin were measured using ELISA kits adhering to the methodology presented by Mellouk et al.30 The target genes Adelin, Apj, and Adiponectin, as well as the internal reference gene  $\beta$ -actin, were subjected to relative quantitative analysis utilizing the real-time PCR system

**Food & Function** 

Light-Cycler 480 from Roche, Germany. Dedicated primer sets (Bioneer, South Korea) developed explicitly for this work are listed in Table 1. The used technique was previously mentioned in detail by Tammam et al.1

All data was analyzed using mean ± SEM. A normal state test was conducted using the SPSS program, version 26, to verify the presence of a normal distribution in the data. Trials with more than two groups and one dependent variable were evaluated for statistical significance using one-way analysis of variance (ANOVA) and post hoc Bonferroni hypothesis testing. Computed Pearson's correlation coefficient was successfully obtained. The criterion for experimental significance (P value) was set at a level lower than 0.05.31

2.2.5. Histopathological examination. A formalin solution that is neutrally buffered was used to fix the excised liver and pancreas of the experimental group for forty-eight hours. They were then rinsed in distilled water and subjected to a progressive sequence of alcohol treatments, followed by a xylene clearing step, and last encased in paraffin wax. Haematoxylin and eosin were used to stain cut sections of 5 micrometers in thickness, subsequently mounted in DPX. The stained sections were analyzed using a light microscope to identify any histological abnormalities. Each field was subjected to an analysis and classified according to the extent of modifications: no (-), slight (+), moderate (++), and significant (+++) damage.<sup>32</sup>

### 2.3. Metabolic profiling C. citratus (DC.) Stapf leaves extract by LC-MS and tandem MS/MS

2.3.1. Chemicals and reagents. Methanol, acetonitrile, and glacial acetic acid were purchased from Fisher Chemicals (HPLC-MS grade) (ThermoFisher, Waltham, MA, USA). Ultrapure water was obtained with a Milli-Q system (Millipore, Bedford, MA, USA).

2.3.2. Analysis by RP-HPLC-ESI-OTOF-MS and -MS/MS. A reversed-phase high-performance liquid chromatography (RP-HPLC) analysis was conducted with an Agilent 1200 series rapid resolution (Agilent Technologies, Santa Clara, CA, USA)

Primer sequence of  $\beta$ -actin, apelin, APJ, and adiponectin Table 1 genes

Target	Sequence
β-Actin	F: 5'-AGGGAAATCGTGCGTGACAT-3'
,	R: 5'-GAACCGCTCATTGCCGATAG-3'
Apelin	F: 5'-TGGAAGGGAGTACAGGGATG-3'
1	R: 5'-TCCTTATGCCCACT-3'
APJ	F: 5'-GGACTCCGAATTCCCTTCTC-3'
·	R: 5'-CTTGTGCAAGGTCAACCTCA-3'
Adiponectin	F: 5'- CTA CTG TTG CAA GCT CTC C-3'
•	R: 5'- CTT CAC ATC TTT CAT GTA CAC C-3'

equipped with a quaternary pump (G7104C) and an autosampler (G7129A). Separation was performed utilizing a Poroshell 120 HiLiC Plus (150 mm × 3 mm, 2.7 μm particle size, Agilent Technologies). The system was coupled to a 6530-quadruple time of flight (Q-TOF) LC/MS (Agilent Technologies) equipped with dual ESI interface according to Mekky et al., 2019, and 2021.33,34 Data analysis and metabolites characterization were done on MassHunter Qualitative Analysis B.06.00 (Agilent Technologies) Mekky et al., 2015, and 2020. 35,36

2.3.3. Statistical analysis. Microsoft Excel 365 (Redmond, WA, USA) was used for statistical analysis, and Minitab 17 (Minitab, Inc., USA).

### 2.4. Preparation of the protein structures and molecular docking (MDock)

The 3D X-ray crystal structure of the apelin receptor (APJ receptor) in complex with the small molecule 8EH ((1R,2S)-N-[4-(2,6dimethoxyphenyl)-5-(6-methylpyridin-2-yl)-1,2,4-triazol-3-yl]-1-(5-methylpyrimidin-2-yl)-1-oxidanyl-propane-2-sulfonamide) was obtained from the Protein Data Bank (PDB ID: 7SUS). PDBQT files were used for docking to the human APJ receptor with AutoDock Vina (version 1.2.3).37 Prior to docking, water molecules, ions, and ligands were removed from 7SUS using AutoDockTools (https://mgltools.scripps.edu/, accessed on 22 May 2024). The 3D structures of the eleven major metabolites from C. citratus leaf extract, as well as the positive control optimized using the RDKit function MMFFOptimizeMolecule with arguments mmffVariant = 'MMFF94' and maxIters = 5000 in Python.<sup>38</sup>The search space coordinates for the APJ receptor (7SUS) were set to encompass the entire macromolecule for docking, with the search space centered at X: -40.361, Y: 5.622, Z: 50.205, and dimensions of X: 20.000, Y: 20.000, Z: 20.000. Ligand tethering to the APJ receptor was achieved by adjusting the genetic algorithm (GA) parameters, utilizing 10 runs of the GA criteria. The docking poses were visualized with the PyMOL Molecular Graphics System (Version 2.0 Schrödinger, LLC), UCSF ChimeraX (version 1.7.1),<sup>39</sup> and the Protein-Ligand Interaction Profiler (PLIP) web tool.40

### 2.5. Physicochemical properties, pharmacokinetic and toxicity profiles and in silico prediction

The physicochemical properties, pharmacokinetic profiles, and toxicity profiles of the 11 major metabolites from C. citratus leaf extract (one amino acid (1), one hydroxycinnamic acid (39), eight flavones (14i, 14ii, 16, 24, 25, 31, 37, 40), and one fatty acid (48)) in our screening library were calculated using the Deep-PK online web tool (https://biosig.lab.uq.edu. au/deeppk/, accessed on 22 May 2024).41 The Deep-PK tool encompasses nine general properties: boiling point (°C), hydration free energy (which indicates the drug's aqueous solubility), log D7.4 (the logarithm of the n-octanol/water distribution coefficient, representing the lipophilicity of a molecule at pH 7.4),  $\log P$  (the logarithm of the *n*-octanol/water distribution coefficient),  $\log S$  (the logarithm of aqueous solubility at a temperature of 20–25 °C), log VP (the logarithm of the

vapor pressure, representing the volatility of a molecule at 25 °C), melting point (°C),  $pK_a$  acid, and  $pK_a$  basic (which control its pharmacokinetic properties).

Seven absorption properties (Caco-2 permeability, Human oral bioavailability, Human intestinal absorption (HIA), Madin–Darby Canine Kidney cells (MDCK) permeability, skin permeability, P-glycoprotein substrate, P-glycoprotein I inhibitor), four distribution properties (BBB (blood–brain barrier) permeability, fraction unbound (human), Plasma protein binding (PPB), Steady State Volume of Distribution (SSVD)), seven metabolism properties (CYP2D6 substrate, CYP3A4 substrate, CYP1A2 inhibitor, CYP2C19 inhibitor, CYP2C9 inhibitor, CYP2D6 inhibitor, CYP3A4 inhibitor), and three excretion properties (total clearance, Half-life, renal OCT2 substrate) were available through the Deep-PK tool.

The 33 available toxicity properties (AMES mutagenesis, avian toxicity, honey bee toxicity, bioconcentration factor, biodegradation, carcinogenicity, crustacean toxicity, liver injury I, liver injury II, eve corrosion and irritation, maximum tolerated dose (human), hERG inhibitor, Daphnia magna toxicity, micronucleus formation, NR-Aryl hydrocarbon Receptor (AhR), NR-Androgen Receptor (AR), NR-Androgen Receptor (AR) Ligand-Binding Domain (LBD) activation, NR-aromatase inhibition, NR-Estrogen Receptor (ER), NR-Estrogen Receptor (ER) Ligand-Binding Domain (LBD), NR-Glucocorticoid Receptor (GR), NR-Peroxisome Proliferator-Activated Receptor Gamma (PPAR-gamma), NR-Thyroid Receptor (TR), oral rat acute toxicity (LD50), oral rat chronic toxicity (LOAEL), Fathead Minnow toxicity, respiratory disease, skin sensitization, SR-Antioxidant Responsive Element (ARE), SR-ATAD5 (ATPase Family AAA Domain Containing 5) gene, SR-Heat Shock Sequence (HSE) elements, SR-Mitochondrial Membrane Potential (MMP), and SR-p53 pathway) in Deep-PK were calculated to predict the potential toxicity profiles of these compounds.

# 3. Results and discussion

# 3.1. *In vivo* deciphering of the anti-obesity properties of *C. citratus* extract

One of the leading causes of cardiovascular diseases is obesity. Systemic metabolic dysfunction and cardiovascular and inflammation problems can result from obesity, which can affect the production of adipokines generated from adipose tissue. 42 Current research indicates that the cardiovascular

systems of overweight rats exhibit dysregulated expression or secretion patterns of Apelin and its receptor, Apj. Apelin system expression was examined in relation to *C. citratus* in this study using overweight rats that were fed a high-carbohydrate, high-fat diet. 42

In Table 2, the comparison between the HCHFD group and the control group revealed a substantial increase (P < 0.05) in fasting blood glucose and HOMA-IR, as well as a substantial decrease (P < 0.05) in insulin level. All other treatment groups revealed a significant reduction (P < 0.05) in fasting blood glucose and HOMA-IR, together with an increase (P < 0.05) in insulin saturation, when compared to the HCHFD group. In addition, there was no discernible difference between the control group and the C. citratus group; nevertheless, there was a striking amount of variation between the groups who received either orlistat alone or in combination with HCHFD. Our findings demonstrate that the group administered HCHFD plus C. citratus demonstrated remarkable improvements in the levels of glucose, insulin, and HOMA-IR.

Indeed, the findings of our study are consistent with previous research, 43 indicating that obese rats experience an accumulation of inflammatory cytokines and free fatty acids in their bloodstream. Deviation from the equilibrium between insulin synthesis and insulin responsiveness might arise when these parameters restrict the uptake and use of glucose in peripheral tissues. This, in turn, leads to high blood glucose levels. As a result of impaired insulin sensitivity, hyperinsulinemia causes the body to create an excess of insulin. On the other hand, insulin production can decline as pancreatic beta cells are fatigued. Inhibition of insulin signaling pathways by inflammatory cytokines generated by adipose tissue can impede the absorption and utilization of glucose-induced by insulin in target tissues. Overweight rats may develop insulin resistance due to a combination of factors, i.e., include dysregulated signaling pathways involved in glucose metabolism, changed adipokine production, modified adipokine secretion from adipose tissue, elevated liberation of free fatty acids from adipose tissue, and chronic low-grade inflammation.1

According to previous studies<sup>44</sup> polyphenols improved glucose absorption by cells, which led us to believe that polyphenols were responsible for the observed decreases in glucose and HOMA-IR levels. The ability to regulate blood sugar levels is conferred upon *C. citratus* by its enhanced glucose absorption, which may improve insulin sensitivity. This discovery lends credence to the research of Adeneye and Agbaje<sup>45</sup> and

Table 2 Measured diabetic parameters in different groups

	Control	HCHFD	C. citratus	HCHFD + C. citratus	HCHFD + Orlistat
Glucose (mg dl <sup>-1</sup> ) Insulin (µIU ml <sup>-1</sup> )	89.44 ± 1.16t 12.91 ± 0.68	$171.47 \pm 2.88^{\text{acd}}$ $9.72 \pm 0.84^{\text{acd}}$	$91.01 \pm 1.2^{\text{bd}}$ $12.85 \pm 0.55^{\text{b}}$	$107.86 \pm 2.85^{abc}$ $11.64 \pm 0.42^{b}$	$127.55 \pm 3.92^{\text{abcd}}$ $10.37 \pm 0.25^{\text{abc}}$
HOMA-IR	$2.84 \pm 0.14$	$4.08 \pm 0.32^{\text{acd}}$	$2.94 \pm 0.15^{\text{b}}$	$3.29 \pm 0.18$ ab	$3.47 \pm 0.12^{ab}$

SE Mean is the statistical distribution used to represent values. For each group, n is the total number of rats, n = 10. A p-value of less than 0.05 was taken to indicate statistical significance. C. citratus group, and HCHFD + C. citratus group at P < 0.05, respectively. a, b, c and d significant when compared to control group, HCHFD group, C. citratus group and HCHFD + C. citratus at P < 0.05, respectively.

Food & Function Paper

Ewenighi et al., which demonstrated that C. citratus restored glucose levels to normal in four weeks of treatment in rats, 46 which demonstrated that C. citratus restored glucose levels to normal in four weeks of treatment in rats.

In comparison to the control group, the HCHFD group exhibited a notable rise (P < 0.05) in triglycerides, LDL-cholesterol, and cholesterol, as well as a notable fall (P < 0.05) in HDL-cholesterol, according to the findings in Table 3.

The results observed in Table 3, showed that as compared to the HCHFD group, all treatment groups had significantly lower levels of cholesterol, triglycerides, and LDL-cholesterol, and significantly higher levels of HDL-cholesterol (P < 0.05). Furthermore, there was considerable fluctuation, but no significant difference, between the control groups and the C. citratus group. Moreover, when comparing the groups given orlistat to those given HCHFD + C. citratus, lipid profiles improved in the groups given orlistat following obesity induction. In contrast, lipid profiles improved significantly in the group given *C. citratus* extract following obesity induction.

It can be concluded that C. citratus extract exhibits hypoglycemic properties.<sup>47</sup> In Wistar rats, a daily dose ranging from 125 to 500 mg per kilogram is found to decrease total cholesterol, HDL, and fasting plasma glucose (FPG). Moreover, C. citratus can be used to treat type 2 diabetes because the dose employed thus far did not exhibit any harm.45 Furthermore, a 4-week course of therapy with C. citratus extracts on diabetic rats' results in decreased blood glucose, TG, cholesterol, and LDL levels. The same procedure caused a decrease in body weight. The essential oils (EO) demonstrated a hypocholesterolemic impact that was mediated via post-transcriptional down-regulation by the regulatory enzyme HMG-CoA reductase. 48 This way, the EO inhibits the hepatic 3-hydroxy-3-methylglutaryl-coenzyme A (HMG-CoA) reductase, which plays a vital role in cholesterol formation.<sup>49</sup>

Additionally, medical practitioners have employed C. citratus to treat neurological diseases associated with etiology. Due to the presence of antioxidant components, it aids in lowering oxidative stress, which is crucial in the development of several neurological disorders. Extracts of C. citratus contain the phenolic chemicals guercetin, gallic acid, guercetin, and rutin. These later offer defense against oxidative stress brought on by several pro-oxidants that cause lipid peroxidation. As a result, C. citratus may be useful in preventing several neurological conditions linked to oxidative stress.<sup>50</sup>

Furthermore, the results in Tables 4 and 5, showed a significant decrease (P < 0.05) in serum apelin, adiponectin, and gene expression of apelin, Apj, and adiponectin when comparing the HCHFD group to the control group. On the other hand, when compared to the HCHFD group, all treatment groups exhibited a substantial rise (P < 0.05) in serum apelin, adiponectin, and gene expression of apelin, Apj, and adiponectin. In addition, there was no discernible difference between the control and C. citratus groups; nevertheless, there was a striking disparity between the orlistat-treated group and the HCHFD + C. citratus group. Both the orlistat and C. citratus groups demonstrated improvements in the apelin system and adiponectin levels following obesity induction, although the citratus extract group exhibited significantly more improvement.

Additionally, the obtained results in Table 5, indicate that apelin's gene expression tends to be lower in circulation levels, which may be related to decreased apelin production in adipose tissue, a significant source of apelin production. It is thought that these alterations are linked to the emergence of insulin resistance and problems resulting from obesity. Insulin sensitivity control has been linked to apelin. In peripheral tissues, including skeletal muscle and adipose tissue, insulin signaling, and glucose uptake can be improved. This

Table 3 Lipid profiles in different groups

	Control	HCHFD	C. citratus	HCHFD + C. citratus	HCHFD + Orlistat
Cholesterol (mg dl <sup>-1</sup> ) Triglyceride (mg dl <sup>-1</sup> )	94.72 ± 1.53 76.53 ± 0.38	169.3 ± 2.19 <sup>acd</sup> 153.07 ± 5.02 <sup>acd</sup>	$94.43 \pm 1.14^{\text{bd}}$ $79.39 \pm 0.95^{\text{bd}}$	$117.76 \pm 1.68^{abc}$ $99.18 \pm 0.49^{abc}$	$143.33 \pm 2.53^{\text{abcd}}$ $116.28 \pm 2.25^{\text{abcd}}$
HDL-cholesterol (mg dl <sup>-1</sup> )	$61.31 \pm 0.37$	$28.27 \pm 0.33^{\text{acd}}$	$63.45 \pm 0.24^{\text{bd}}$	$51.23 \pm 0.89^{abc}$	$45.70 \pm 0.64^{abcd}$
LDL-cholesterol (mg dl <sup>-1</sup> )	$22.30 \pm 1.56$	$96.42 \pm 3.44^{\text{acd}}$	$21.10 \pm 1.75^{\mathrm{bd}}$	$46.70 \pm 2.19^{abc}$	$74.37 \pm 2.76^{abcd}$

SE Mean is the statistical distribution used to represent values. For each group, n is the total number of rats, n = 10. A p-value of less than 0.05 was taken to indicate statistical significance. C. citratus group, and HCHFD + C. citratus group at P < 0.05, respectively. a, b, c and d significant when compared to control group, HCHFD group, C. citratus group and HCHFD + C. citratus at P < 0.05, respectively.

Table 4 Serum levels of apelin and adiponectin in different groups

Con	itrol F	HCHFD	C. citratus	HCHFD + C. citratus	HCHFD + Orlistat
I ( 0 )	.03 ± 2.16 1	$134.21 \pm 2.71^{\text{acd}}$ $6.49 \pm 0.28^{\text{acd}}$	172.88 ± 1.95 <sup>bd</sup> 16.18 + 0.34 <sup>bd</sup>	$158.95 \pm 2.13^{abc}$ $11.94 \pm 0.38^{abc}$	$141.67 \pm 1.80^{\text{abcd}} \\ 8.55 \pm 0.22^{\text{abcd}}$

SE Mean is the statistical distribution used to represent values. For each group, n is the total number of rats, n = 10. A p-value of less than 0.05 was taken to indicate statistical significance. C. citratus group, and HCHFD + C. citratus group at P < 0.05, respectively. a, b, c and d significant when compared to control group, HCHFD group, C. citratus group and HCHFD + C. citratus at P < 0.05, respectively.

Table 5 The mRNA fold change of the expression of apelin, Apj and adiponectin genes by RT-qPCR in different groups

	Control	HCHFD	C. citratus	HCHFD + C. citratus	HCHFD + Orlistat
Apelin Apj	$1.00 \pm 0.00$ $1.00 \pm 0.00$	$0.43 \pm 0.02^{\ acd} \ 0.39 \pm 0.04^{acd}$	$\begin{array}{l} 1.31 \pm 0.08^{abd} \\ 1.25 \pm 0.06^{abd} \end{array}$	$0.64 \pm 0.01^{\mathrm{abc}} \ 0.71 \pm 0.01^{\mathrm{abc}}$	$0.57 \pm 0.02^{\mathrm{abcd}} \ 0.64 \pm 0.04^{\mathrm{abcd}}$
Adiponectin	$\boldsymbol{1.00 \pm 0.00}$	$0.33 \pm 0.01^{\rm acd}$	$1.52 \pm 0.07^{abd}$	$0.57 \pm 0.01^{abc}$	$0.46 \pm 0.01^{ m abcd}$

implies that apelin plays a part in controlling how glucose is metabolized and how insulin resistance develops.<sup>51</sup> Furthermore, the expression of the APJ receptor is frequently changed in obesity, albeit the direction of the shift varies according to the tissue or cell type. For instance, APJ receptor expression may be downregulated in adipose tissue, which could explain why apelin signaling is less effective in this tissue. It has been demonstrated that apelin affects immunological response and inflammation. It can control the synthesis and release of several inflammatory chemokines and cytokines. Apelin may act in a pro- or anti-inflammatory manner.<sup>52</sup>

Our results contradicted the findings of other research that indicated a significant increase in obesity was associated with serum apelin levels and its genes. Obese humans and animals have high concentrations of plasma apelin. Boucher *et al.*, demonstrated in 2005 that apelin was secreted and produced by adipocytes, as well as that apelin and insulin had a close association both *in vivo* and *in vitro*. In the adipose tissue (AT) of obese animal models, apelin expression rose in tandem with hyperinsulinemia. Additionally, they found that apelin level and body mass index were positively correlated. Since obesity-related elevations in inflammatory cytokines can hasten apelin production and release.

Moreover, Adiponectin is a protein that is particular to adipocytes and increases the sensitivity of the liver and muscle to the effects of insulin. 55,56 Numerous studies indicate that adiponectin has anti-atherosclerotic, anti-insulin resistance, and anti-inflammatory characteristics.<sup>57</sup> Adiponectin appears to have anti-inflammatory and protective metabolic qualities that prevent atherosclerosis, and it may be a marker for coronary artery disease.<sup>58</sup> A significant decrease in adiponectin during obesity was observed due to the ability of adiponectin to increase the oxidation of free fatty acids, insulin effectiveness, decrease gluconeogenetic enzymes, enhance phosphorylation of acetyl Co-A carboxylase, enhance the production of certain cytokines, and enhance the metabolism of glucose and lactate. In conclusion, adiponectin, has significant anti-diabetic benefits.<sup>59</sup> Similarly, adiponectin was observed to be lower in obese rats compared to controls; however, following treatment with C. citratus, there was an increase in serum adiponectin levels.60

In accordance with our findings, Chakraborti proposed that increased TNF- $\alpha$  and IL-6 production, a hypoxic microenvironment created in larger adipocytes, and increased production of insulin-like growth factor binding protein-3 which

is obesity-induced and inhibits adiponectin transcription could be the cause of the reduction in adiponectin in obesity.<sup>61</sup>

In particular, *C. citratus* has been investigated for possible impacts on adipocyte metabolism and function; in obese rats, it may help restore normal function of the adipose tissue by encouraging apelin and adiponectin synthesis, release, and gene expression. *C. citratus* may affect insulin sensitivity, according to certain research. <sup>62</sup>*C. citratus* may indirectly affect the levels and functionality of these variables by increasing insulin sensitivity in obese rats. <sup>63</sup> Additionally, *C. citratus* includes a variety of antioxidant chemicals, including flavonoids and phenolic compounds. APJ receptor, apelin, adiponectin, and adiponectin gene expression can all be negatively impacted by oxidative stress in terms of production and signaling. In obese rats, the antioxidant qualities of *C. citratus* may help lower oxidative stress and maintain normal levels and functioning of these variables. <sup>64</sup>

Furthermore, an enzyme known as AMP-activated Protein Kinase (AMPK) is essential for energy metabolism and the control of several metabolic functions, including apelin synthesis and release, APJ receptor function, adiponectin, and adiponectin gene expression, according to some research, *C. citratus* active biocomponents can activate AMPK, which could aid obese rats' levels and functionality of these variables.<sup>63</sup>

Pearson's correlation was calculated for the concerned parameters along the studied groups as shown in Fig. 1 and 2 as well as Table S1.† Where the calculated correlation showed a statistically positive correlation in apelin when correlated with adiponectin, apelin gene, APJ, adiponectin gene, and HDL, r was 0.865, 0.826, 0.836, 0.774, and 0.889, respectively. In contrast, it showed a negative correlation with cholesterol, TG, LDL, and glucose; r was -0.898, -0.881, -0.883, and 0.829, respectively. Moreover, a statistically significant positive correlation was observed when correlating adiponectin with the apelin gene, APJ, adiponectin gene, and HDL, r was 0.846, 0.849, 0.852, and 0.921, respectively. However, it showed a negative correlation with cholesterol, TG, LDL, and glucose, r was -0.940, -0.892, -0.931, and -0.882 respectively.

Herein, apelin has an inverse relationship with glucose, HOMA-IR, cholesterol, TG, and LDL but a direct relationship with insulin, HDL, Apj, and adiponectin. Additionally, adiponectin has an inverse relationship with glucose, HOMA-IR, cholesterol, TG, and LDL but a direct relationship with insulin, HDL, Apj, and apelin. Accordingly, it can be con-

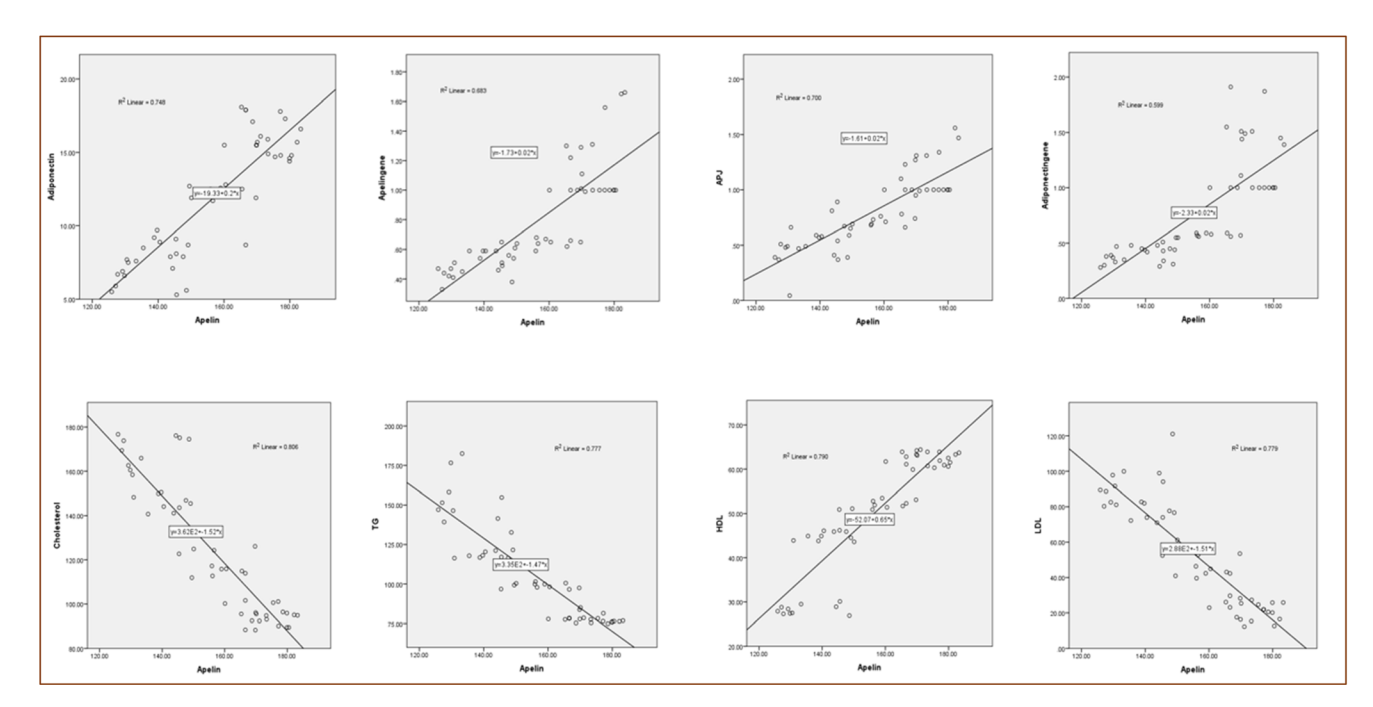


Fig. 1 Pearson's correlation chart of apelin with the other parameters in the studied groups.

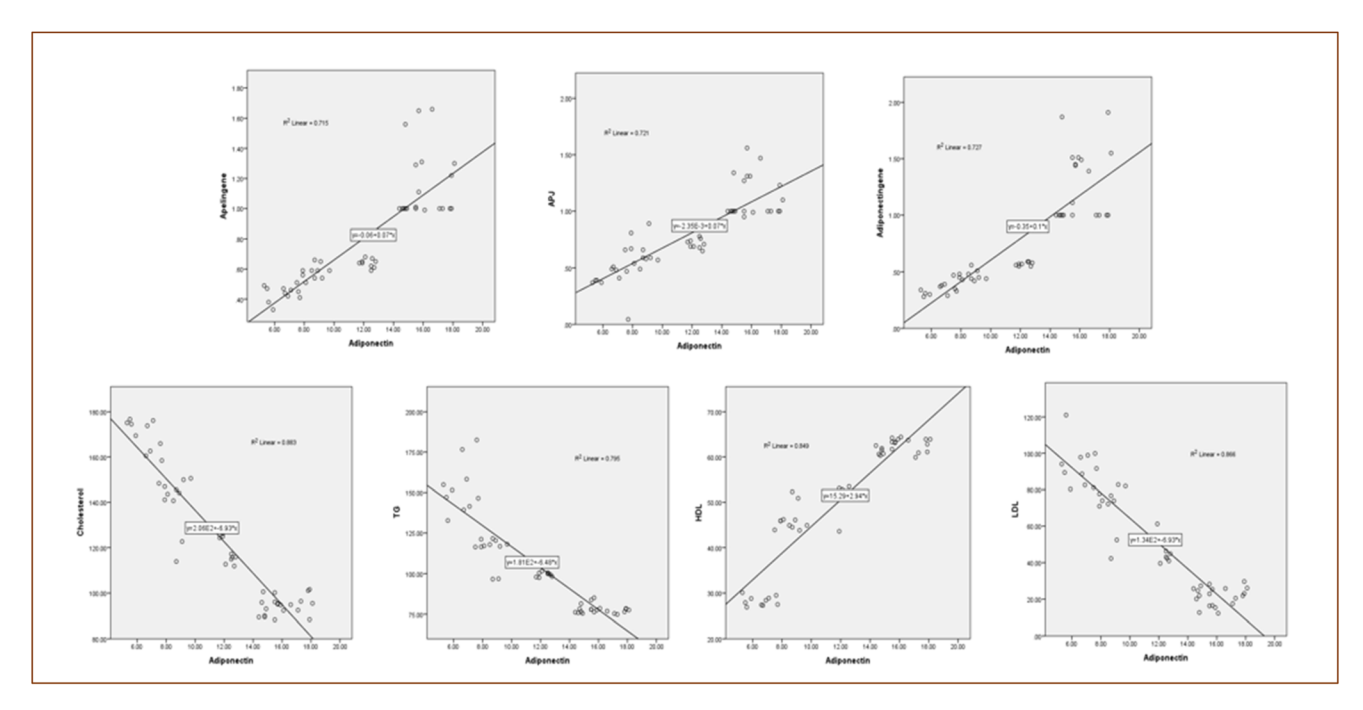


Fig. 2 Pearson's correlation chart of adiponectin with the other parameters in the studied groups.

cluded that apelin and adiponectin may have a strong correlation with lipid profile levels, insulin resistance, and cardiovascular health *via* different pathways.

The obtained results of the histological examination supported our biochemical results (Fig. 3 and 4), which demonstrated that the sections of liver from the control group dis-

played normal hepatic architecture features, such as rounded vesicular nuclei with blood sinusoids and hepatocytes arranged in cords radiating from the central veins (Fig. 3a).

On the other hand, while histological analysis of the liver tissues from the HCHFD group revealed fatty cells, necrosis, focal infiltration of mononuclear cells with pyknotic nuclei,

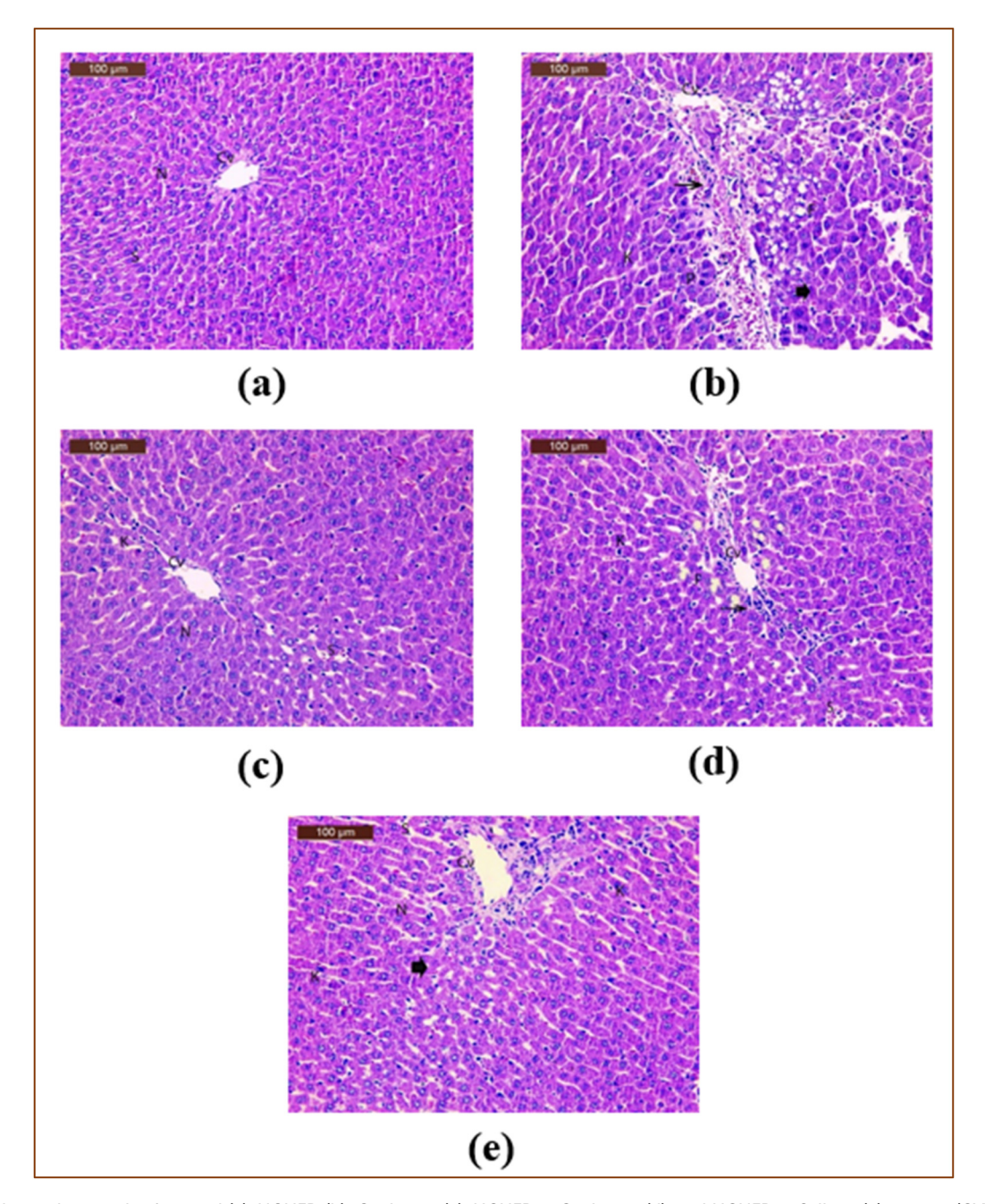


Fig. 3 Liver photomicrograph of control (a), HCHFD (b), *C. citratus* (c), HCHFD + *C. citratus* (d), and HCHFD + Orlistat (e) groups; (CV): central vein; (S): blood sinusoids; (N): nucleus; (arrowhead): necrosis; (F): fatty cells; (arrow): mononuclear cell infiltration; (P): pyknotic nuclei; and (K): Kupffer cells.

degenerative alterations surrounding the major vein, and modest activation of Kupffer cells (Fig. 3b), *C. citratus* displayed almost normal structure in group C, along with a slight initiation of Kupffer cells (Fig. 3c). The hepatic tissues belonging to HCHFD + *C. citratus* group, showed virtually normal structure with minor activation of Kupffer cells, mononuclear cell infiltration, slightly dilated blood sinusoids with few pyknotic nuclei, and slight degenerative alterations around the central vein (Fig. 3d). A section of the hepatic tissue from the HCHFD + Orlistat group revealed minor activation of Kupffer

cells, a few adipose cells with pyknotic nuclei within slightly dilated blood sinusoids, and nearly normal structure coupled with degenerative alterations around the major vein (Fig. 3e).

In terms of the pathological analysis of the pancreatic sections that were taken, the sections from the control group demonstrated normal histoarchitecture and islets of Langerhans (Islets) with pale, ovoid, rounded  $\beta$ -cells implanted in the exocrine region of the pancreas (Fig. 3a). In contrast, the sections from the HCHFD group revealed disorganization in the endocrine and exocrine glands, shrunken islets of

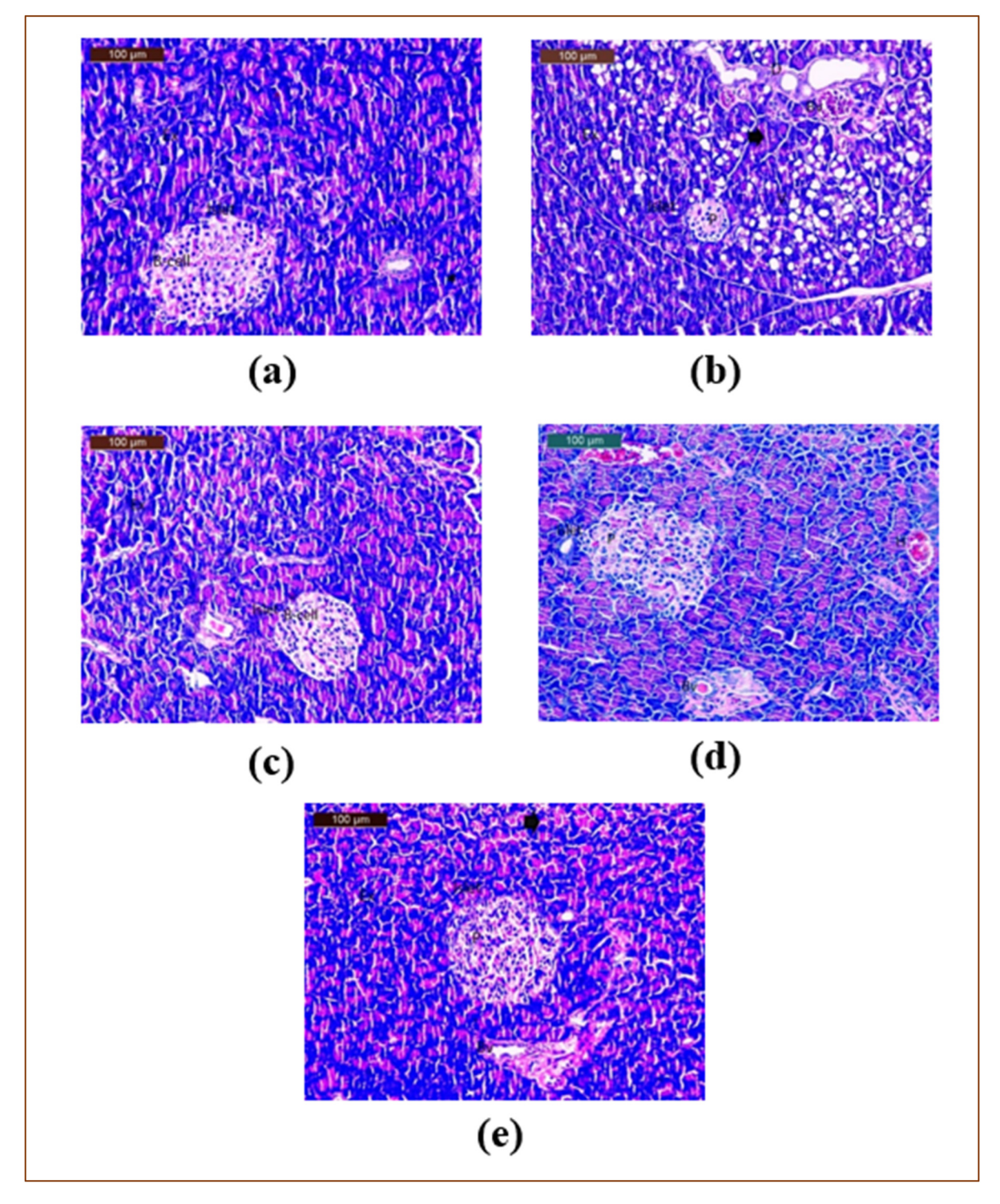


Fig. 4 Pancreas photomicrograph of control (a), HCHFD (b), C. citratus (c), HCHFD + C. citratus (d), and HCHFD + Orlistat (e) groups; (Islet): islets of Langerhans; (V): vacuolation; (arrowhead): necrosis; (Ex): degeneration exocrine acini; (D): ductal slight dilatation; (Bv): congestion blood vessels; (P): pyknotic nuclei; and (H): interstitial haemorrhage.

Langerhans (Islets), visible degeneration and necrosis of the islet-making cells, vacuolation, exocrine acini's degeneration, fatty changes, and ductal slight dilatation surrounded by mildly infiltrating inflammatory cells (Fig. 4b). Furthermore, the pancreatic slices from the *C. citratus* group showed nearly

normal islet organization, with exocrine acini and  $\beta$  cells positioned in the center (Fig. 4c). Furthermore, interstitial bleeding and congestion were seen in some blood arteries, and the pancreatic sections from the HCHFD + *C. citratus* group showed normal islets of Langerhans, despite the detection of

some cells with small pyknotic nuclei in the islet's canter, some of which were still degenerating, and nearly normal exocrine acini (Fig. 4d). The objective is to restore the typical structure of the pancreas, which consists of pancreatic islets of a typical size with few pyknotic nuclei and almost normal exocrine acini, was another indication of a somewhat improved pancreatic tissue structure in the HCHFD + Orlistat group's examination results (Fig. 4e). However, some of the clogged blood arteries were still degenerating.

# 3.2. Metabolic profiling *C. citratus* (DC.) Stapf leaves extract by LC-MS and tandem MS/MS

*C. citratus* (DC.) Stapf leaves extract profiling utilizing RP-HPLC-MS and tandem MS/MS in the negative and positive ionization mode portrayed the presence of 52 metabolites. Within this particular framework, Fig. 5a, illustrates the base peak chromatogram of the extract. The characterization approach of the metabolites was based on observations of retention times (RT), derived molecular formulas, double bond equivalence (DBE), molecular ion peaks (m/z), neutral losses, and peak areas (Fig. 5b), as described in earlier publications,  $^{65,66}$  consulting relevant literature and databases.  $^{8,9,67-69}$  In total, 52 metabolites were detected (Fig. 5

and 6, Table 6), the annotated metabolites were grouped into flavones (27, Fig. S1–S3), hydroxycinnamic acids (10, Fig. S4), hydroxybenzoic acid (1, Fig. S5), fatty acids (8, Fig. S6), amino acids (4, Fig. S7), an organic acid (1, Fig. S8), and a diterpenoid (1, Fig. S9†).

As for flavones, they were derivatives of luteolin, luteolin O-methyl ether (Fig. S5), apigenin (Fig. S6), and tricin (Fig. S7†). They represented the major class of annotated metabolites with 27 derivatives qualitatively and 61.51% of the relative abundance (Table 6). In this regard, two constitutional isomers of apigenin hexoside deoxyhexoside were observed with  $m/z = 577.16^{-}/579.17^{+}$  and molecular formula  $C_{27}H_{30}O_{14}$ and yet both showed different fragmentation patterns where the first isomer exhibited the C-glycosylation pattern with neutral loss of n CHOH groups of  $(n \times 30 \text{ Da})$ , 66 whereas the second one exerted the neutral loss of a hexosyl and a deoxyhexosyl moieties and hence they were described as apigenin C-hexoside deoxyhexoside and apigenin O hexoside deoxyhexoside that were mentioned in the family Poaceae as vitexin 2"-Orhamnoside and apigenin-7-O-β-D-rutinoside, respectively. 68 Indeed, advanced methods such as RP-HPLC-ESI-OTOF-MS and -MS/MS enabled the distinction of constitutional isomers with closely related chemical formulae. Similarly, peak 15 showed a C-glycosylation pattern and the characteristic frag-

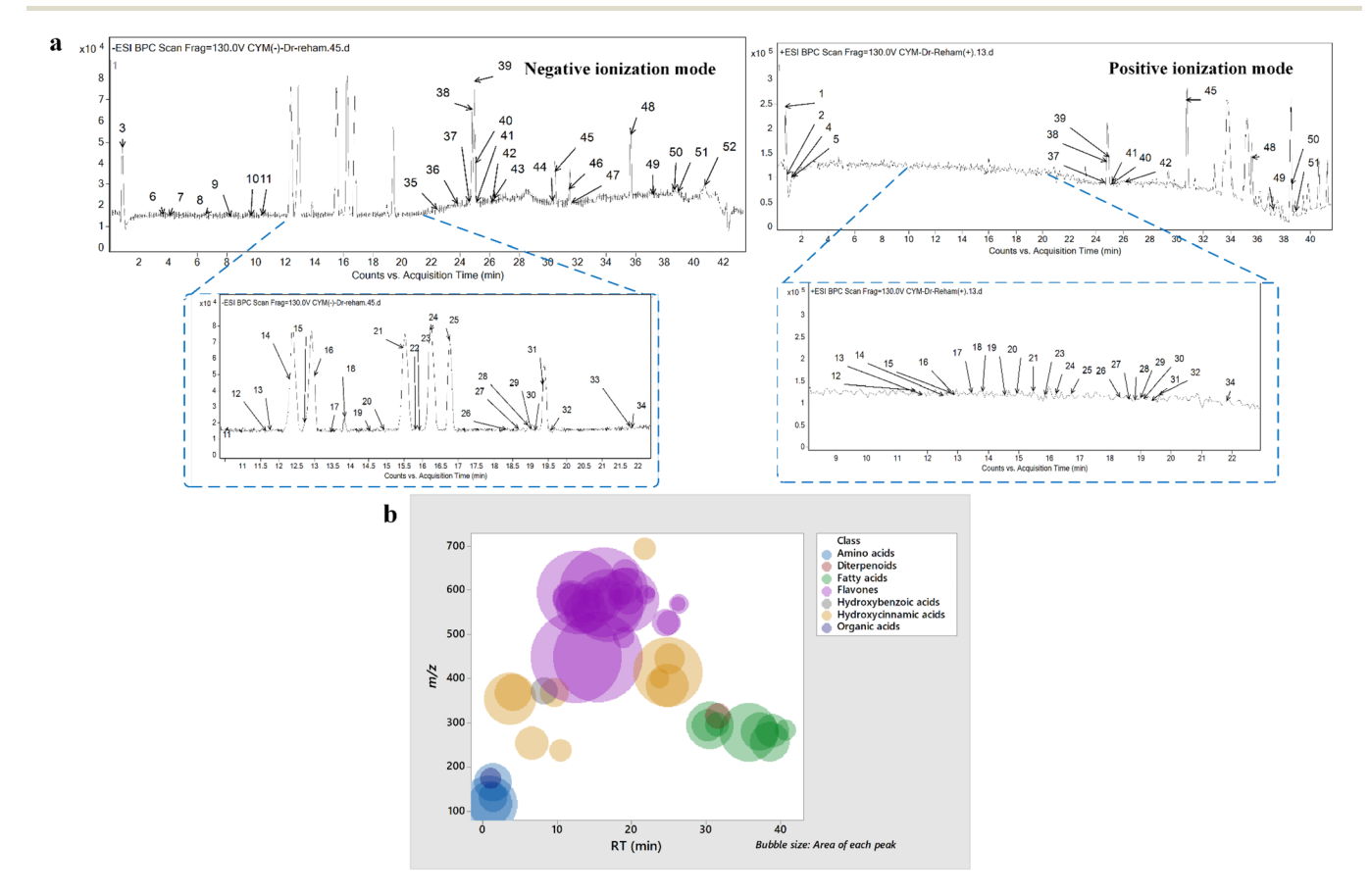


Fig. 5 (a) Base peak chromatograms (BPCs) of the *C. citratus* leaves extract in the negative and positive ionization mode, and (b) bubble plot of the observed masses *m/z vs.* the retention time concerning metabolites classes and peak areas.

Fig. 6 Structures of the major characterized metabolites in C. citratus.

ment ion 117.03 [1,3B], and hence it was characterized as apigenin C-pentoside hexoside which was identified as isoschaftoside in C. citratus<sup>68</sup> (Table 6, and Fig. S10a†). Regarding luteolin derivatives, 15 glycosides were noticed, with a relative abundance of about 53% of the total characterized metabolites. They exhibited O-glycosylation, characterized by the neutral loss of the sugar moiety, resulting in the formation of the aglycone at m/z = 285.04, <sup>33</sup> and *C*-glycosylation where the loss of *n* CHOH (30 Da) groups occurred, 34 alongside the characteristic fragment ions of [1,3A], [1,3B], and [0,2B] which were noticed at m/z = 151, 133 and 135, respectively.<sup>70</sup>

In this sense, two constitutional isomers of C<sub>21</sub>H<sub>20</sub>O<sub>11</sub> were characterized as luteolin C hexoside and luteolin O hexoside (Fig. S10b†) according to their fragmentation pattern (Table 6) where they described in C. citratus as orientin/isoorientin and luteolin 7-O-glucoside.<sup>68</sup> In the same manner, peaks 16, 19, and 24 were characterized as luteolin C hexoside deoxyhexoside isomers I-II (Fig. S10c†) and luteolin O-hexoside deoxyhexoside, respectively. It bears noting that they were mentioned in C. citratus as isoorientin 2"-O-rhamnoside and luteolin 7-neohesperidoside.<sup>68</sup> Luteolin C dipentoside isomers I-II were characterized (Table 6). They were described in the family Poaceae as Kurilensin B (Luteolin 6 C (2-O-(β-D-xylopyranosyl)α-L-arabinofuranosyl)).68 Likewise, peak 25 was annotated as luteolin C-deoxyhexoside pentoside that was observed in C. citratus as Kurilensin A,68 (Table 6). Additionally, two isomers of luteolin C hexoside pentoside I-II and luteolin C di-deoxyhexoside I-II were detected in C. citratus extract that

This article is licensed under a Creative Commons Attribution-NonCommercial 3.0 Unported Licence. Open Access Article. Published on 25 November 2024. Downloaded on 3/10/2025 9:26:47 AM. (cc) BY-NC

Table 6 A list of 52 metabolites characterized in C. citratus leaves extract

%	$0^5 \ 3.53$ $0^5 \ 2.13$		$0^{\circ} 1.49$ $0^{\circ} 0.9$		$0^5$ 1.44		$0^5 0.71$ $0^5 0.88$	$0^4   0.54$	$0^5 1.09$	$0^5 1.35$	80.6 <sup>9</sup> 0	0 <sup>5</sup> 2.03	06 7.7	04 0.52	0 <sup>5</sup> 1.89	$0^4   0.37 $ $0^4   0.44$	0 <sup>6</sup> 8.73	$0^4 0.22$	$0^5 2.12$	0 <sup>6</sup> 8.76	05 5.76	$0^4   0.47$ $0^4   0.56$	04 0.44	0 <sup>5</sup> 1.37
Area	$5.00 \times 10^5$ $3.02 \times 10^5$	$5.91 \times 10^4$	$2.12 \times 10^{5}$ $1.27 \times 10^{5}$	$4.07\times10^5$	$2.04\times10^5$	$1.72 \times 10^5$	$1.01 \times 10^5$ $1.25 \times 10^5$	$7.70 \times 10^{4}$	$1.54\times10^5$	$1.91\times10^5$	$1.29\times10^{6}$	$2.88\times10^5$	$1.09\times10^{6}$	$7.38 \times 10^4 0.52$	$2.69 \times 10^5$	$5.20 \times 10^4$ $6.28 \times 10^4$	$1.24\times10^6$	$3.16\times10^4$	$3.01\times10^5$	$1.24\times10^{6}$	$8.17\times10^5$	$6.64 \times 10^4$ $7.93 \times 10^4$	$6.23\times10^4$	$1.94\times10^5$
Class	Aa Aa	Oa	Aa	HC	HC	HC	HB	HC	됴	됴	댐	됴	표	됴	표	댐댐	FI	됴	됴	댐	됴	표표	됴	됴
DBE Proposed compound	Proline Valine	Dehydroascorbic acid	Phenylalanine Leucine/Isoleucine	Caffeoylquinic acid	3-O-Feruloylquinic acid I	1-0-caffeoylglycerol	1-O-benzoyl-3-α-glucuronosylglycerol 3-O-Feruloylquinic acid II	1-0-p-coumaroy glycerol	Luteolin C hexoside pentoside (Carlinoside) I	Luteolin $C$ hexoside pentoside (Carlinoside) II	Luteolin C hexoside	Apigenin C-pentoside hexoside (Isoschaftoside)	Luteolin C hexoside deoxyhexoside I	Luteolin C di pentoside I	Luteolin C di pentoside II	Luteolin <i>C</i> hexoside deoxyhexoside II Apigenin <i>C</i> hexoside deoxyhexoside	Luteolin O hexoside	Diosmetin C hexoside deoxyhexoside	Luteolin $C$ di deoxyhexoside I	Luteolin O hexoside deoxyhexoside	Luteolin C deoxyhexoside pentoside (Kurilensin A)	Apigenin O hexoside deoxyhexoside Luteolin O methylether C dideoxyhexoside (2"- O-alpha-t-Rhamnosyl-6-C-fucosyl-3'- methoxylureoiin) I	Tricin-O-hexoside	Diosmetin O hexoside deoxyhexoside (Diosmin)
DB	1		1 5	∞	8	9		9	13	13	12	13	13	13	13	13	12	13	13	13	13	13	15	13
Main fragments	71.0651, 70.0685 N.D.	111.0103	121.0859, 105.0699, 104.0592, 103.541 N.D.	191.0551, 179.0364, 173.0435, 135.0476	193.0502, 191.0570, 149.0574,	134.0366 $179.0333, 161.0245, 135.0446$	249.0626, 121.0285, 103.0401, 77.0401 193.0465, 173.0450, 149.0587,	134.0374 163.0414, 145.0294, 119.0498	561.1212, 519.1113, 489.1026, 459.0923, 429.0827, 399.0711, 369.0608. 133.0270	489.1018, 459.0934, 399.0705, 369.0596, 133.0437	429.0848, 369.0622, 357.0507, 327.0572, 297.0396, 133.0300	545.1256, 503.1167, 473.1084, 443.0972, 383.0770, 353.0670, 117.0362	575.1412, 503.1192, 473.1090, 429.0823, 369.0616, 309.0400, 133.0297	489.1058, 459.0891, 429.0822, 399.0729, 369.0607, 339.0489, 133.0272	489.1041, 459.0927, 429.0808, 399.0709, 369.0611, 339.0490, 133.0235	503.1156, 473.0986, 383.0735 457.1133, 413.0869, 353.0660,	285.0453, 284.0313, 151.0030,	133.0273 487.1281, 433.0983, 383.0713, 353.0637, 323.0542	473.1070, 457.1140, 415.1033, 353.0667, 311.0557, 285.0377, 133.053	447.0896, 285.0400, 284.0313, 151.0051. 133.0317	545.1308, 503.1175, 473.1081,357.0610, 327.0499, 133.0372	415.0921, 269.0452 487.1252, 367.0876, 325.0652	329.0641, 329.0597, 314.0429, 313.0367, 299.0179, 285.0351, 271.0230, 227.0268	461.1002, 299.0554, 285.0360, 284.0330, 255.0296
Error (mDa)	-0.6	0.6	0.3	-0.2	0-	0	1.7	0	-0.2	0.3	-0.4	-0.2	0.3	-0.4	0.7	0.7	0.3	0.3	1.1	-0.1	0.4	1.4	0	0.7
Error (ppm)	-5.3 -2.5	3.4	1.5	9.0-	-0.1	0.1	4.5	-0.2	-0.4	9.0	6.0-	-0.4	0.4	-0.7	1.3	0.8	9.0	0.5	1.8	-0.1	9.0	2.4	0	1.2
E Score (	85.29 -		97.92 86.79		82.32	97.77	73.02 73.32	86.53 -	93.65 -	95.26	- 8.85	98.83 -	77.79	96.46 -	96.15	97.04 96.07 -	90.66	93.84	95.21	- 66	99.41	90.39	- 8.76	98.58
Molecular formula	$\mathrm{C_5H_9NO_2} \\ \mathrm{C_5H_{11}NO_2}$	C <sub>6</sub> H <sub>6</sub> O <sub>6</sub>	C <sub>9</sub> H <sub>11</sub> NO <sub>2</sub> C <sub>6</sub> H <sub>13</sub> NO <sub>3</sub>	$C_{16}H_{18}O_9$	$\mathrm{C}_{17}\mathrm{H}_{20}\mathrm{O}_{9}$	$\mathrm{C}_{12}\mathrm{H}_{14}\mathrm{O}_{6}$	$C_{16}H_{20}O_{10}$ $C_{17}H_{20}O_{9}$	$C_{12}H_{14}O_5$	$C_{26}H_{28}O_{15}$	$C_{26}H_{28}O_{15}$	$C_{21}H_{20}O_{11} \\$	$C_{26}H_{28}O_{14}$	$C_{27}H_{30}O_{15}$	$C_{25}H_{26}O_{14}$	$C_{25}H_{26}O_{14}$	$C_{27}H_{30}O_{15}$ $C_{27}H_{30}O_{14}$	$C_{21}H_{20}O_{11}$	$C_{28}H_{32}O_{15}$	$C_{27}H_{30}O_{14}$	$C_{27}H_{30}O_{15}$	$C_{26}H_{28}O_{14}$	$C_{27}H_{30}O_{14}$ $C_{28}H_{32}O_{14}$	$C_{23}H_{24}O_{12}$	$C_{28}H_{32}O_{15}$
Ionization [M] Mode	115.064 P 117.0797 P	_	165.079 P 131.0949 P	354.095 N	368.1102 N		372.1053 N 368.1102 N	238.0836 N	580.143 N/P	580.143 N/P	448.1006 N/P	564.1478 N/P	594.1585 N/P	550.1326 N/P	550.1326 N/P	594.1585 N/P 578.1647 N/P	448.1006 N/P	608.1738 N	578.1647 N/P	594.1585 N/P	564.1478 N/P	578.1647 N/P 592.1794 N/P	492.1264 N/P	608.1738 N/P
[M + H] <sup>+</sup>	116.0712		166.086 132.102		Ē			- 1	581.1511	581.1496	449.1088	565.1558	595.1667	551.1407	551.1397	595.1656 579.1714	449.1091		601.1541 <sup>a</sup>	595.1669	565.156	$579.1708$ $615.1686^a$		
[M – H] <sup>-</sup>	1	173.0084		353.0875	367.1034	253.0719	371.0977 367.1029	237.0768	579.1353 5	579.1351 5	447.0937 4	563.1409 5	593.1516 5	549.1253 5	549.1246 5	593.1509 5 577.1558 5	447.0932 4	607.1674	577.1553 6	593.1514 5	563.1404 5	577.1555 5 591.1707 6	491.1186 493.1338	607.1661 609.1826
RT (min) [	0.79		1.28		4.06		8.25 3 9.65 3	10.4	11.62 5	11.78 5	12.53 4	12.72 5	12.89 5	13.43 5	13.8 5	14.57 5 14.88 5	15.48 4	15.74 6	15.87 5	16.21 5	16.7 5	18.33 5 18.63 5	18.88 4	19 6
Peak J	1 2	.3	4 5	9	7	8	9 10		12	13	14	15	16	17	18	20	21	22	23	24	25	26	78	29

											- >								. =
%	$1.02 \times 10^5 0.72$	$6.59 \times 10^5 4.65$	$1.29 \times 10^5 0.91$	4 0.54	4 0.35	$5.21 \times 10^4 0.37$	$1.04 \times 10^5 0.73$	5 2	5 5.29	$7.89 \times 10^4 0.56$	$1.30 \times 10^5 0.92$ $2.69 \times 10^4 0.19$		5 2 37				5 1.56		4 0.46
g	2 × 10	9 × 10	9 × 10	$7.63 \times 10^4$	$4.93 \times 10^4$ $1.75 \times 10^4$	11 × 10	14 × 10	$2.83 \times 10^5$	$7.51 \times 10^5$	9 × 10	$\frac{1.30 \times 10^5}{2.69 \times 10^4}$	$5.30 \times 10^{4}$	$1.51 \times 10^{3}$	$8.08 \times 10^{4}$	$9.26 \times 10^{4}$	$5.34 \times 10^{3}$	$2.22 \times 10^{3}$	$1.58 \times 10^{5}$	$6.52 \times 10^4$
Class Area	1.0	6.5	1.2		1.7		1.0			7.8		5.3							6.5
Ü	FI	된	뎐	HC	E.".	HC	됴	HC	НС	FI	HC Fl	됴	Fa G	Fa	Σţ	Fa	E E	Fa	Fa
DBE Proposed compound	Tricin O-hexoside deoxyhexoside	Cassiaoccidentalin B	Luteolin $C$ di deoxyhexoside $\Pi$	Di-O-feruloylsucrose	3'-O-Methylmaysin Luteolin O methylether C dideoxyhexoside (2"- Oalpha-t-Rhamnosyl-6-C-fucosyl-3'- methoxyluteolin) II	O-Coumaroyl-O-caffeoylglycerol	Tricin 4'-O-(β-guaiacyl-glyceryl)ether I	Di-O-coumaroylglycerol	O-Coumaroyl-O-feruloylglycerol	Tricin 4′-O-(β-guaiacyl-glyceryl)ether II	Di-O-feruloylglycerol Tricin O-phenylhexoside I	Tricin O-phenylhexoside II	Hydroxylinolenic acid I	Hydroxylinoleic acid	Gibberellin A9	Linolenic acid	Linoleic acid Palmitic acid	Oleic acid	Stearic acid
DBE	13	14	13	14	14 14	12	15	12	12	15	12 16	16	4 <	* co	8	4	ω <del>-</del>	5	1
Main fragments	475.0888, 329.0654, 314.0421, 299.0151, 271.0262	577.1291, 531.1129, 455.0949, 411.0711, 367.0454, 337.0351, 133.0278	487.1211, 413.0859, 353.0640, 341.0643, 285.0583, 135.0087	449.1439, 337.0912, 193.0507, 175.0392, 149.0588	425.0887, 365.0641, 299.0535 N.D.	253.0711, 179.0327, 163.0386, 161.0244, 145.0307, 135.0445, 119.0500	329.0674, 314.0419, 299.0194, 271.0204, 227.0268, 195.0662, 180.0408, 165.0553	237.0757, 163.0390, 145.0284, 119.0497	237.0739, 193.0499, 175.089, 163.0394, 149.0606, 145.0286, 119.0500	329.0663, 314.0418, 299.0209, 271.0162, 180.0385, 165.0549	193.0496, 175.0400, 149.0589 329.0652, 314.0421, 299.0202, 255.0380	329.0666, 314.0445, 299.0191	275.2016, 231.2132	277.2171, 233.2191	278.8683, 234.5192	259.2098, 233.2279	261.2192 237 2273	263,2211	N.D.
Error (mDa)	1.3	0.2	0.1	6.0	0.2	0.5	0	0.1	0.1	0.2	0.1	0	-0.3	0.1	0.7	0.1	0.2	0	6.0
Error (ppm)	2.1	0.4	0.2	1.3	0.3	1.2	0	0.3	0.4	0.3	0.3	0.2	-1.1	0.5	2.1	0.3	0.7	-0.1	3.2
Error Score (ppm)	89.27	94.13	98.18	97.58	80.63	98.85	97.8	62.96	97.19	76.93	99.34 97.67		96.18	82.23	89.3	97.82	93.32		92.74
Molecular formula	$C_{29}H_{34}O_{16}$	$C_{27}H_{28}O_{14}$	$C_{27}H_{30}O_{14}$	$C_{32}H_{38}O_{17}$	$C_{28}H_{30}O_{14}$ $C_{28}H_{32}O_{14}$	$C_{21}H_{20}O_8$	$C_{27}H_{26}O_{11}$	$\mathrm{C}_{21}\mathrm{H}_{20}\mathrm{O}_7$	$\mathrm{C}_{22}\mathrm{H}_{22}\mathrm{O}_8$	$C_{27}H_{26}O_{11}$	$C_{23}H_{24}O9$ $C_{29}H_{28}O_{12}$	$C_{29}H_{28}O_{12}$	$C_{18}H_{30}O_3$	$C_{18}H_{32}O_{3}$	$\mathrm{C}_{19}\mathrm{H}_{24}\mathrm{O}_4$	$C_{18}H_{30}O_2$	$C_{18}H_{32}O_{2}$	$C_{18}H_{34}O_{2}$	$\mathrm{C}_{18}\mathrm{H}_{36}\mathrm{O}_{2}$
Ionization [M] Mode	5 638.1852 N/P	576.1476 N/P	7 578.1647 N/P	694.2102 N	4 590.1645 N/P 592.1794 N	400.1155 N	525.1404 549.1391 <sup>a</sup> 526.1474 N/P	$383.1137 407.1106^a 384.1208 \text{ N/P}$	413.1241 437.1216 <sup>a</sup> 414.1321 N/P	525.1404 527.1569 526.1474 N/P	443.1345 467.1321 <sup>a</sup> 444.1419 N/P 567.1505 591.1488 <sup>a</sup> 568.1598 N/P	568.1598 N	294.2211 N 5a 204 2211 N/D	296.2364	316.1678	278.2264	3 280.2413 N/P 2 256.246 N/P	282.2559	284.2724 N
M + H]	539.192	577.156	579.1717		591.171		549,139	107.110	137.1210	527.156	$467.1321^a$ $591.1488^a$		217 2005			279.2325	281.2483	283.264	
$[M - H]^- [M + H]^+$	637.1764 639.1925	575.1401 577.156	577.156 5	693.2028	591.1751 591.1714	399.108	525.1404	383.1137 4	413.1241 4	525.1404 5	443.1345 4 567.1505 5	567.1502	293.2128				279.2327 2		283.2634
RT (min)	19.1	19.36	19.56	21.74	21.84	23.71	24.54	24.78	24.91	25.02	25.11 26.2	26.35	30.27	31.49	31.61	35.74	37.21	38.88	40.71
Peak no.	30	31	32	33	34	36	37	38	39	40	41	43	44	46	47	48	49	51	52

were described as luteolin 6-C- $\beta$ -D-glucopyranoside-8-C- $\alpha$ -L-arabinopyranoside and in C. citratus and as luteolin 8-C-rhamnoside-7-O-rhamnoside, respectively. <sup>68</sup> Peak 31, with a molecular formula  $C_{27}H_{28}O_{14}$  and  $m/z=575.14^-/577.16^+$  expressed C-glycosylation fragmentation pattern and hence was tentatively characterized as cassiaoccidentalin B (luteolin C-6-deoxy-2-O-(6-deoxy- $\alpha$ -L-mannopyranosyl)- $\beta$ -L-ribo-hexopyranos-3-ulosyl). <sup>68</sup>

Concerning luteolin *O*-methyl ether (diosmetin) derivatives, two isomers of luteolin *O* methylether ( $C_{28}H_{32}O_{14}$ ) were conjugated with two deoxyhexosides in a *C*-glycosylation pattern and hence were characterized as luteolin *O*-methylether *C*-dideoxyhexoside isomers I–II which were described in *Zea mays* as (2"-O- $\alpha$ -L-rhamnosyl-6-C-fucosyl-3'-methoxyluteolin). Besides, peak 34 with m/z 589.16 $^-/5$ 91.17 $^+$  and molecular formula  $C_{28}H_{30}O_{14}$  was annotated as 3'-O-methylmaysin. Sea In this concern, two constitutional isomers with molecular formula  $C_{28}H_{32}O_{15}$  exhibited different fragmentation patterns for C-glycosylation and O-glycosylation and were characterized as Luteolin O methyl ether C hexoside deoxyhexoside which was identified as 2"-O- $\alpha$ -L-rhamnosyl-4'-O-methylorientin (Fig. S11a) and diosmetin O-hexoside deoxyhexoside, which was described as diosmin (Fig. S11b†). 67

With regards to tricin derivatives, their presence was described for the first time in C. citratus, 67,68 in this regard, tricin O-hexoside, tricin O-hexoside deoxyhexoside were observed exerting the neutral loss of the conjugated sugar with the appearance of the ion of tricin m/z = 329.06 followed by the sequential loss of two methyl moieties (15 Da  $\times$  2). <sup>67,68</sup> Furthermore, peaks 42 and 43 showed the neutral loss of a phenylhexoside moiety (238 Da) followed by the typical fragmentation of tricin. Consequently, they were characterized as tricin O-phenylhexoside I-II, considered new proposed structures. As a matter of fact, the occurrence of phenylhexoside was described in the family Poaceae as phenyl β-D-glucopyranoside. 68 Moreover, two isomers of tricin 4'-O-(β-guaiacyl-glyceryl) ether I-II were noticed with neutral loss of guaiacyl-glyceryl moiety (196.08 Da) and tricin fragmentation pattern and the appearance of guaiacyl glyceryl m/z = 195.07 and guaiacyl glyceryl –CHOH m/z = 165.06 (Fig. S11c†). It bears noting that they were described in *Zizania latifolia*, in the family Poaceae.<sup>67</sup>

The occurrence of hydroxycinnamic acids was mainly as coumaric acid, caffeic acids and the *O*-methylated derivatives of the latter as ferulic acid derivatives. The aforementioned derivatives are either conjugated with glycerol, quinic acid, or sugars. The conjugation is mono hydroxycinnamic acid or dihydroxycinnamic acid (Table 6). Peak 11, in this context, displayed the neutral loss of a glyceryl moiety (74 Da) followed by the characteristic fragmentation pattern of coumaric acid. The fragmentation pattern began with the molecular ion of coumaric acid at m/z = 163.04, followed by its dehydrated and decarboxylated ions at m/z = 145.3 and 119.05, consecutively, <sup>34,66</sup> and hence it was characterized as 1-*O-p*-coumaroyl glycerol which was described in the family Poaceae. <sup>67</sup> In the same manner, peak 38 with  $m/z = 383.11^-/407.11^+$  (ion sodium adduct) exhibited a similar fragmentation pattern to the com-

pound above with an additional neutral loss of a coumaroyl moiety. Consequently, it was characterized as di-O-coumaroyl glycerol. Also, peak 8 showed a neutral loss of a glyceryl moiety followed by caffeic acid ion m/z=179.03 alongside its dehydrated and decarboxylated ions at m/z=161.02 and 135.04, respectively. It was characterized as 1-O-caffeoylglycerol. The Moreover, peaks 36 and 39 portrayed a glycerol moiety neutral loss followed by the fragmentation pattern of coumaric acid and caffeic acid for the former one and ferulic acid for the latter one, and hence they were tentatively identified as O-coumaroyl-O-caffeoyl glycerol (Fig. S12a and Table 6) and O-coumaroyl-O-feruloyl glycerol (Fig. S12b† and Table 6). Accordingly, peak 41 with  $m/z=443.13^-/467.13^+$  (ion with sodium adduct) and molecular formula  $C_{23}H_{24}O_9$  was characterized as di-O-feruloyl glycerol.  $C_{19}$ 

In line with quinic acid conjugates with hydroxycinnamic acid, caffeoyl quinic acid and feruloyl quinic acid isomers I–II were noticed in *C. citratus* extract, figuring out the ions of m/z 191.05 and m/z = 173.04 accounting for quinic acid and quinic acid-H<sub>2</sub>O accompanied with either caffeic acid or ferulic acid fragmentation (Table 6).  $^{33,34,67,69}$ 

Furthermore, peak 33 with m/z = 639.20- and molecular formula  $C_{32}H_{38}O_{17}$  exhibited the neutral loss of feruloyl moiety as well as two hexosyl moieties with the presence of a ferulic acid fragmentation pattern (Fig. S3c†). Therefore, it was annotated as di-*O*-feruloyl sucrose.<sup>67</sup>

Regarding hydroxybenzoic acid, it is noteworthy that peak 10 with  $m/z = 377.10^-$  showed the neutral loss of benzoic acid with the appearance of benzoic acid ion m/z = 121.03 as well as its dehydrated (m/z = 103.04) and decarboxylated (m/z = 77.03) fragments and was identified as 1-*O*-benzoyl-3- $\alpha$ -glucuronosyl glycerol (Fig. S13a†).<sup>67</sup>

The presence of palmitic acid (C16:0) and stearic acid (C18:0) was seen in conjunction with the unsaturated isomers of the latter, namely oleic acid (C18:1), linoleic acid (C18:2), and linolenic acid (C18:3). Moreover, hydroxylinoleic acid (Fig. S13b†) and hydroxylinolenic acid isomers I–II were also detected (Table 6). Four amino acids were present in *C. citratus* extract, namely proline, valine, phenylalanine, and leucine/isoleucine, in agreement with previous studies. S13c† Besides, gibberellin A9 and dehydroascorbic acid (Fig. S13c†) were detected (Table 6).

# 3.3. Molecular docking (MDock), binding energies studies and structure-activity relationships (SARs) analysis

Molecular docking was utilized to examine the binding interactions of eleven major metabolites derived from *C. citratus* leaf extract with the human APJ protein (PDB ID: 7SUS), aiming at treating obesity. The dataset of metabolites from *C. citratus* includes: one amino acid (1), one hydroxycinnamic acid (39), eight flavones (14i, 14ii, 16, 24, 25, 31, 37, 40), and one fatty acid (48), as depicted in Fig. 6 and Table 7, presents the outcomes of molecular docking conducted using AutoDock Vina software on the APJ protein.

As shown in Table 7, the metabolites with the lowest calculated  $\Delta G_{\rm B}$  values, indicating the most promising candidates,

**Table 7** Calculated free binding energies ( $\Delta G_{\rm B}$ , in kcal mol<sup>-1</sup>) and the detailed interactions established upon docking the eleven metabolites from *C. citratus* and the positive control, **8EH**, Tyr271, Phe291 Trp85, Phe291 π-Stacking residues Arg168, Lys268, Ser298 Ser105, Arg168, Tyr185, Tyr264, Iyr88, Arg168, Tyr185, Lys268 Iyr93, Arg168, Tyr264, Ser298 Arg168, Tyr264, Lys268 Arg168, Tyr264, Ser298 Arg168, Lys268, Ser298 Arg168, Try264, Ser298 Iyr93, Arg168, Ser298 H-bond residues Met183 Trp85, Ile109, Phe110, Val267, Lys268, Tyr271, Trp85, Ile109, Tyr264, Tyr271, Phe291, Thr295 Phe78, Trp85, Tyr88, Trp95, Ile109, Thr295, Phe110, Tyr264, Tyr271, Phe291, Tyr299 lle109, Phe110, Tyr264, Phe291, Pro292, Ne109, Tyr271, Phe291, Thr295, Tyr299 rp85, Ile109, Tyr264, Thr295 Prp85, Tyr93, Ile109, Tyr299 Hydrophobic residues Prp85, Ile109, Thr295 Thr295, Tyr299 de109, Tyr182 Tyr93, Tyr271 Interaction Phe291 -8.44-8.16-8.24-6.32-9.00-9.47-9.01-10.02Pricin-4'-O-(erythro-beta-guaiacylglyceryl) ſricin-4'-O-(erythro-beta-guaiacylglyceryl) Luteolin C 6-hexoside deoxyhexoside I Luteolin C 6-deoxyhexoside pentoside Juteolin O 7-hexoside deoxyhexoside O-Coumaroyl-O-feruloylglycerol **8EH** (triazole derivative) Luteolin C 8-hexoside 2 Luteolin C 6-hexoside Cassiaoccidentalin B Linolenic acid Kurilensin A) ether II ether I Proline Name 14ii 16 24 25 48 37 40 Hydroxycinnamic Positive Control $^b$ against APJ Amino acid Fatty acids acid Flavones Class

are flavones with a luteolin C6-glycosylation core featuring two sugar units. Specifically, luteolin C 6-deoxyhexoside pentoside (25), luteolin C 6-hexoside deoxyhexoside I (16), and cassiaoccidentalin B (31) have estimated  $\Delta G_{\rm B}$  values less than or equal to -9 kcal  ${\rm mol}^{-1}$ , with precise values of -9.01, -9.47, and -10.02 kcal  ${\rm mol}^{-1}$ , respectively. It is also worth noting that the positive control (8EH), a known ligand of the APJ protein, has a calculated  $\Delta G_{\rm B}$  value of -9 kcal  ${\rm mol}^{-1}$ . As shown in Fig. 7, the best-docked pose for the positive control (8EH), was demonstrated on APJ protein.

In Fig. 8, the best-docked poses for the three most probable lead-like anti-obesity APJ inhibitors, **16**, **25** and **31**, were shown. These excellent binding affinities could be attributed to potential hydrogen bond interactions with the residue Arg168 of the APJ protein, both in the positive control (Fig. 7) and in the three flavone derivatives proposed as anti-obesity agents (Fig. 8).

For example, in the three flavones with a luteolin *C*-6-glyco-sylation core featuring two sugar units (**16**, **25**, and **31**), there appear to be hydrogen bond interactions between the oxygen atom of the hydroxyl group at position 5 of the benzene ring (ring A) for **16**, the hydroxyl group at position 7 of the benzene ring (ring A) for **25**, or the oxygen atom of the carbonyl group of the heterocyclic pyran ring (ring C) for **31** of the 4*H*-chromen-4-one core, and the two amine groups of the guanidino moiety of the residue Arg168. The length of the hydrogen bonds varies specifically, for **16**: 2.38 and 2.46 Å; for **25**: 2.61 Å; and for **31**: 2.27 and 3.19 Å.

# 3.4. Pharmacokinetics, toxicity and druglikeness (ADME/Tox), *in silico* prediction

<sup>1</sup> In keal mol<sup>-1</sup>. b(1R,2S)-N-f4-(2,6-Dimethoxyphenyl)-5-(6-methylpyridin-2-yl)+1,2,4-triazol-3-yl]-1-(5-methylpyrimidin-2-yl)-1-oxidanyl-propane-2-sulfonamide, APJ ligand.

To examine the physicochemical properties, pharmacokinetic profiles, and toxicity profiles of the 11 principal metabolites derived from *C. citratus* leaf extract (comprising one amino acid (1), one hydroxycinnamic acid (39), eight flavones (14i, 14ii, 16, 24, 25, 31, 37, 40), and one fatty acid (48)) in our screening library, we utilized a freely available online tool called Deep-PK (https://biosig.lab.uq.edu.au/deeppk/, accessed on May 22, 2024). The tool was employed to analyze their profiles, and the results are detailed in Table S2 in the ESI.† Table 8 presents the physicochemical and ADMET properties of our most promising metabolites, specifically the three flavones with a luteolin *C6*-glycosylation core featuring two sugar units (16, 25, and 31).

The log *D*7.4, the logarithm of the *n*-octanol/water distribution coefficient, represents the lipophilicity of a molecule at pH 7.4, impacting both aqueous solubility and membrane permeability. For un-ionizable compounds, log *P* and log *D*7.4 values will be similar. The optimal range for log *P* and log *D*7.4 in orally administered drugs is between 1 and 3.<sup>41</sup> All three flavone derivatives and the positive control are predicted to have lower lipophilicity at pH 7.4 (<1). However, the flavone derivative (31) and the positive control (8EH) are predicted to possess adequate pH-independent lipophilicity characteristics. Additionally, all three derivatives and the positive control are predicted to have adequate water solubility characteristics.

Paper Food & Function

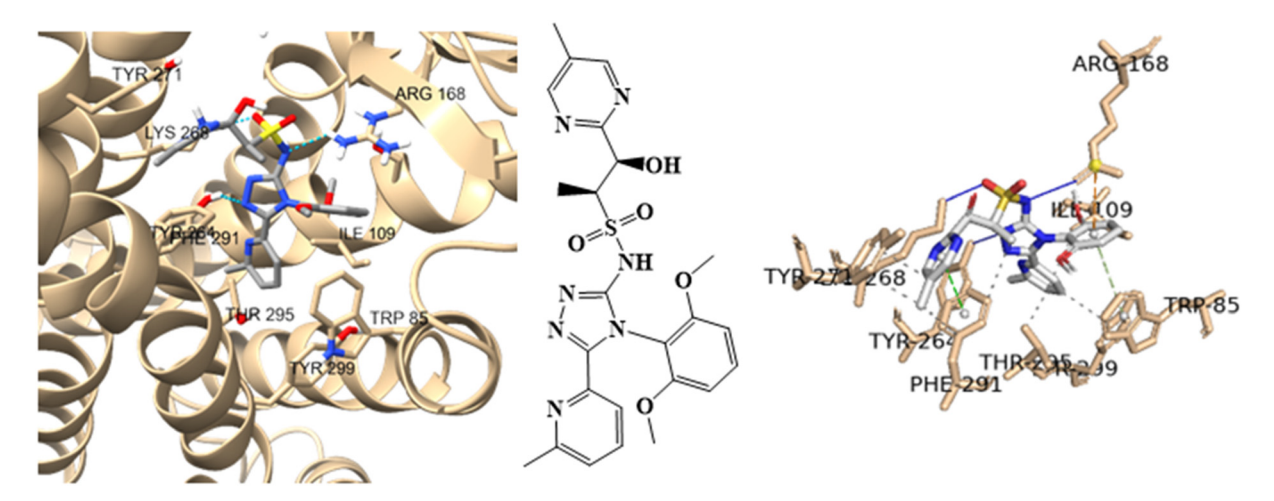


Fig. 7 Interaction profile of the best-docked pose for the positive control, 8EH, against APJ. The hydrophobic interactions are shown as black dash lines and the  $\pi$ -stacking interactions in green (parallel) and gray (perpendicular) dash lines.

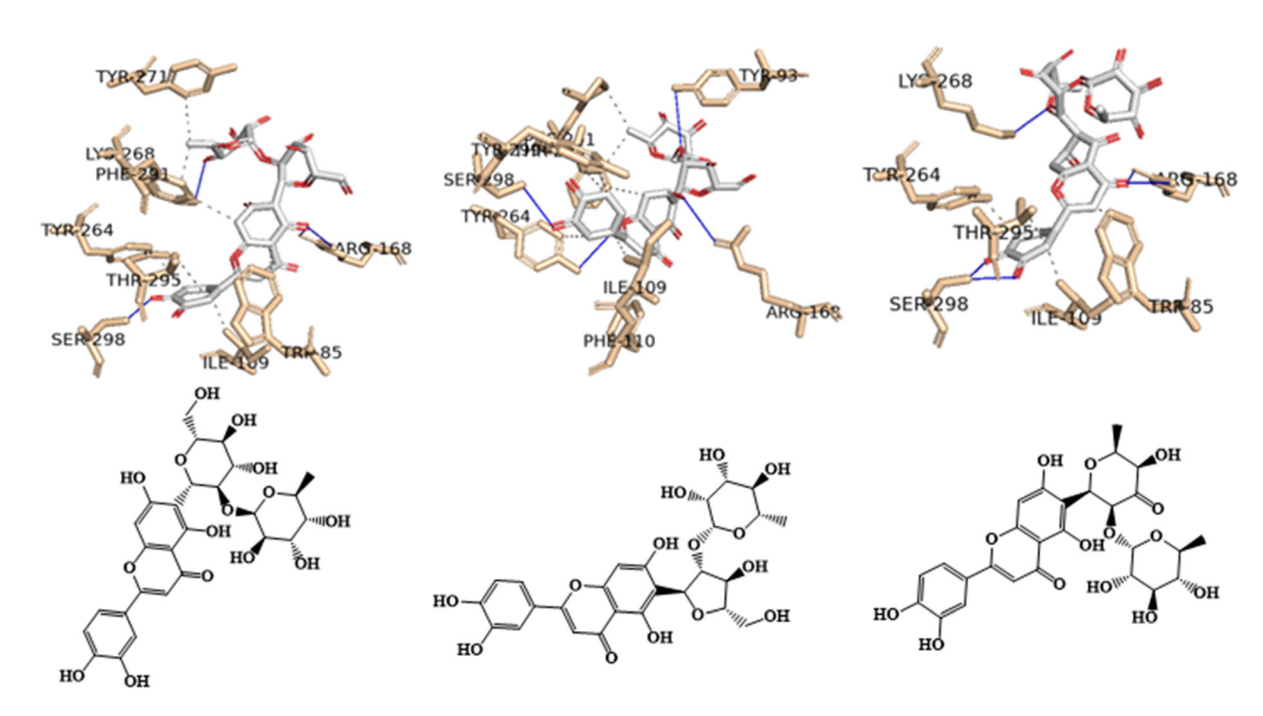


Fig. 8 Interaction profile of the best-docked pose for the three most probable anti-obesity APJ inhibitors, 16, 25 and 31. The hydrophobic interactions are shown as black dash lines and the  $\pi$ -stacking interactions in green (parallel) and gray (perpendicular) dash lines.

The Caco-2 cell monolayer is widely used as an *in vitro* model of the human intestinal mucosa to predict the absorption of orally administered drugs. Low Caco-2 permeability was predicted for all three flavone derivatives (16, 25, and 31) as well as the positive control (8EH). However, only the positive control was estimated to be human oral bioavailable and human intestinally absorbed, whereas the three flavones were predicted to be neither bioavailable nor absorbed. In terms of skin permeability, the behavior is reversed: the three flavone derivatives are predicted to have high skin permeability, while the positive control is predicted to have low skin permeability.

All flavone derivatives (16, 25, and 31) and the positive control (8EH) are estimated to be poorly distributed to the brain. However, an appropriate value for plasma protein binding, which is a therapeutic index related to the amount of free drug in the body, was predicted for all the compounds. Only the positive control (8EH) was predicted to have a low value for the steady-state volume of distribution (SSVD), which is related to drug concentration.

All flavone derivatives (16, 25, and 31) are estimated to be non-inhibitors of cytochrome P450 isoforms (CYP1A2, CYP2C19, CYP2C9, CYP2D6, CYP3A4), an important class of detoxification enzymes primarily found in the liver.

Table 8 ADME/Tox profiling of three selected flavone derivatives and the positive control (8EH)

		Flavones			Pariti a contra
	ADME/Tox	16	25	31	Positive contro <b>8EH</b>
General Properties	$\log D7.4$	-0.730	-0.180	0.420	0.890
•	$\log P$	0.360	0.830	1.410	1.990
	$\log S$	-4.330	-4.500	-5.170	-3.380
Absorption	Caco-2 permeability	-6.430	-6.480	-6.710	-5.390
1	Human Oral Bioavailability 20%	$NB^a$	$NB^a$	$NB^a$	$\mathrm{B}^b$
	Human Intestinal Absorption	$NA^c$	$NA^c$	$NA^c$	$\mathbf{A}^d$
	Skin Permeability	7.170	3.880	3.670	-2.360
Distribution	Blood-Brain Barrier	$\mathrm{NP}^e$	$\mathrm{NP}^e$	$\mathrm{NP}^e$	$\mathrm{NP}^e$
	Plasma Protein Binding	68.160	73.840	82.060	86.650
	$\mathrm{SSVD}^f$	0.940	0.940	1.010	0.560
Metabolism	CYP 1A2, CYP 2C19, CYP 2D6, OATP1B1 Inhibitor	$\mathbf{NI}^g$	$NI^g$	$NI^g$	$NI^g$
	CYP 1A2, CYP 2C19, CYP 2D6 Substrate	$\mathrm{NS}^h$	$\mathrm{NS}^h$	$NS^h$	$NS^h$
	CYP 2C9, CYP 3A4 Inhibitor	$NI^g$	$NI^g$	$NI^g$	$\mathbf{I}^i$
	CYP 2C9, CYP 3A4 Substrate	$\mathrm{NS}^h$	$\mathrm{NS}^h$	$\mathrm{NS}^h$	$\mathbf{S}^{j}$
Excretion	Clearance	11.380	13.170	14.470	1.390
	Organic Cation Transporter 2	$\mathbf{NI}^g$	$NI^g$	$NI^g$	$NI^g$
Toxicity	AMES Mutagenesis	Toxic	Toxic	Toxic	Safe
•	Avian	Safe	Safe	Safe	Safe
	Bee	Safe	Toxic	Toxic	Toxic
	Biodegradation	Safe	Safe	Safe	Safe
	Carcinogenesis	Safe	Safe	Safe	Safe
	Crustacean	Safe	Safe	Safe	Toxic
	Liver Injury I	Safe	Safe	Safe	Safe
	Eye Corrosion	Safe	Safe	Safe	Safe
	Eye irritation	Safe	Safe	Safe	Safe
	Maximum Tolerated Dose	0.770	0.780	0.820	0.960
	Liver Injury II	Toxic	Toxic	Toxic	Toxic
	hERG Blocker	Safe	Safe	Safe	Safe
	Skin Sensitization	Safe	Toxic	Toxic	Safe

<sup>&</sup>lt;sup>a</sup> Non-Bioavailable. <sup>b</sup> Bioavailable. <sup>c</sup> Non-absorbed. <sup>d</sup> Absorbed. <sup>e</sup> Non-penetrable. <sup>f</sup> Steady state volume of distribution. <sup>g</sup> Non-inhibitor. <sup>h</sup> Non-substrate. <sup>i</sup> Inhibitor. <sup>j</sup> Substrate.

In terms of toxicity predictions, all flavone derivatives (16, 25, and 31) are predicted to be toxic in the AMES mutagenicity test, indicating potential mutagenicity and, therefore, possible carcinogenicity. However, all flavone derivatives (16, 25, and 31) are also predicted to be non-carcinogenic. Only flavone (16) and the positive control (8EH) were predicted not to cause skin sensitization.

## 4. Conclusions

Obesity represents a critical and immediate global public health issue, imposing a significant burden in terms of both disability and mortality. The current study found that HCHFD rats had reduced apelin, Apj and adiponectin expression, and that treatment with *C. citratus* greatly enhanced these changes, leading to improvements in insulin resistance, body weight, inflammatory markers, lipid profile, serum apelin, adiponectin and insulin levels. *C. citratus* treatment of overweight rats led to weight loss, improved insulin resistance and inflammatory markers, and upregulation of the Apelin axis. Besides, *C. citratus* was subjected to untargeted metabolic profiling *via* RP-HPLC-QTOF-MS and MS/MS disclosing the presence of 52 metabolites where they mainly belonged to phenolic compounds *viz.*, flavones and hydroxycinnamic acids, among other

metabolites. Additionally, a molecular docking was utilized to examine the binding interactions of eleven major metabolites derived from C. citratus leaf extract with the human APJ protein (PDB ID: 7SUS), aiming at treating obesity, where the best-docked poses for the three most probable lead-like antiobesity APJ inhibitors, 16, 25 and 31, were shown. These excellent binding affinities could be attributed to potential hydrogen bond interactions with the residue Arg168 of the API protein, both in the positive control and in the three flavone derivatives proposed as anti-obesity agents. Moreover, the pharmacokinetic, physicochemical, and toxicity profiles of the 11 major metabolites from C. citratus leaf extract were evaluated, uncovering a profile similar to that of the positive control in the three selected flavone metabolites. Based on these findings, C. citratus may represent a new regulator of the Apelin axis, which could alleviate some of the problems associated with obesity in a rat model.

# Ethics approval

All procedures were conducted in accordance with the UK Animals (Scientific Procedures) Act, 1986 and related guidelines, EU Directive 2010/63/EU for animal experiments, and the National Research Council's Guide for the

Paper			Food & Function
Care and Use of	Laboratory Animals. The animal study	kcal/mol	Kilocalorie per mole
	proved by the Ethics Committee of	LBD	Ligand-binding domain
National Research	Center, Dokki, Cairo, Egypt, approval	LC-MS	Liquid chromatography-mass
number (01542082	4).		spectrometry
		$\mathrm{LD}_{50}$	Oral rat acute toxicity
		LDL	Low density lipoprotein
Abbreviation	IS	LOAEL	Oral rat acute toxicity
		$\log D7.4$	The logarithm of the <i>n</i> -octanol/water dis-
2-ΔΔCt method	The delta-delta Ct method		tribution coefficient, representing the
Aa	Amino acids		lipophilicity of a molecule at pH 7.4
ADME/Tox	Pharmacokinetics, toxicity and	$\log P$	The logarithm of the <i>n</i> -octanol/water dis-
	druglikeness		tribution coefficient
AhR	NR-Aryl hydrocarbon receptor	$\log S$	The logarithm of aqueous solubility at a
AlCl <sub>3</sub>	Aluminum trichloride	1	temperature of 20–25 °C
AMPK	AMP-activated Protein Kinase	log VP	The logarithm of the vapor pressure,
ANOVA	One-way analysis of variance		representing the volatility of a molecule
APJ	Apelin receptor genes	) (D CV	at 25 °C
APLN	Apelin	MDCK	Madin-darby canine kidney cells
AR	NR-androgen receptor	MDOCK	Molecular docking
ARE	SR-antioxidant responsive element Adipose tissue	MIQE	Minimum information for publication of
AT	Blood-brain barrier	MMD	quantitative real-time PCR experiments
BBB BPCs		MMP N	SR-mitochondrial membrane potential Nucleus
Bv	Base peak chromatograms Congestion blood vessels	N.D.	Not detected
ъv С.	Cymbopogon	Oa	Organic acids
cDNA	Complementary DNA	P	Pyknotic nuclei
CV	Central vein	PCR	Polymerase chain reaction
D	Ductal slight dilatation	PDBQT	An extended protein data base (PDB)
DBE	Double bond equivalence	IDDQI	format for coordinate files, incorporating
Dt	Diterpenoid		atomic partial charges and atom types
ELISA	The enzyme-linked immunosorbent	PLIP	Protein-ligand Interaction Profiler
	assay	PPAR-gamma	NR-peroxisome proliferator-activated
EO	Essential oils	<b>6</b>	receptor gamma
ER	NR-estrogen receptor	PPB	Plasma protein binding
Ex	Degeneration exocrine acini	qPCRTM	Real-time polymerase chain reaction
Fa	Fatty acids	RP-HPLC	Reversed-phase high-performance liquid
FI	Flavones		chromatography
FPG	Fasting plasma glucose	RP-HPLC-QTOF-MS	Reversed-phase high-performance liquid
GA	Genetic algorithm		chromatography coupled with quadru-
GR	NR-glucocorticoid receptor		pole-time-of-flight mass spectrometry
Н	Interstitial haemorrhage	S	Blood sinusoids
НВ	Hydroxybenzoic acids	SAR	Structure-activity relationship
HC	Hydroxycinnamic acids	SPSS	Statistical software suit
HCHFD	High-carbohydrate, high-fat diet	SR-ATAD5	ATPase Family AAA Domain Containing
HDL	High density lipoprotein		5
HIA	Human intestinal absorption	SSVD	Steady state volume of distribution
HMG-CoA	Hepatic 3-hydroxy-3-methylglutaryl-coen-	SYBR Green I®	Asymmetrical cyanine dye
	zyme A	T-chol	Total cholesterol
HOMA ID formula	Homogetatic model assessment for	TC	Trickyooridaa

HOMA-IR formula Homeostatic model assessment for insulin resistance

 $TNF\text{-}\alpha$ performance liquid

High chromatography SR-heat shock sequence

Interleukin 6 Islets of Langerhans Kupffer cells

TR **UPLC-Orbitrap** 

TG

V

 $\Delta G_{
m B}$ 

HRMS

NR-Thyroid Receptor Ultra-high-performance liquid chromatography

Triglycerides

Tumor necrosis factor

high-resolution

spectrometry Vacuolation

Free binding energy

**HPLC** 

**HSE** 

IL-6

Islet

K

mass

# **Author contributions**

Conceptualization: M.A.T and A-E.D.; methodology: O.A., R.H. M., F.P., M.A.T., and A-E.D.; software: O.A., R.H.M., and F.P.; formal analysis: O.A., R.H.M., and F.P., investigation: O.A., R. H.M., F.P., M.A.T., and A-E.D.; resources: Y.M.D.; data curation: O.A., R.H.M., F.P., M.A.T., and A-E.D.; writing original draft preparation: O.A., R.H.M., F.P., M.A.T., and A-E.D.; writing review and editing: O.A., R.H.M., F.P., M.A.T., and A-E.D.; visualization: M.A.T and A-E.D. All authors have read and agreed to the published version of the manuscript.

# Data availability

The data presented in this study are available in the present article and the ESI.†

# Conflicts of interest

The authors declare that they have no known competing commercial interests or personal relationships that could have appeared to influence the work reported in this paper.

# Acknowledgements

Florbela Pereira gratefully acknowledges FCT – Fundação *para* a Ciência e a Tecnologia, I. P., for an Assistant Research Position (CEECIND/01649/2021) and the project UIDB/50006/2020 of the Associated Laboratory for Green Chemistry (LAQV) of the Network of Chemistry and Technology (REQUIMTE). Mohamed A. Tammam is humbly dedicating this work to the soul of his sister Dr Mai A. Tammam who passed away on 19 of March 2022, she was always a kind supporter in all aspects of his life. Amr El-Demerdash is thankful to his home universities, University of East Anglia (UK) and Mansoura University (Egypt) for the unlimited support, inside and outside.

## References

- 1 M. A. Tammam, O. Aly, F. Pereira, A. Mahdy and A. El-Demerdash, Unveiling the potential of marine-derived diterpenes from the order Alcyonacea as promising antiobesity agents, *Curr. Res. Biotechnol.*, 2024, 7, 100175.
- 2 B. Shokrollahi, H. Y. Zheng, L. Y. Li, L. P. Tang, X. Y. Ma, X. R. Lu, A. Q. Duan, Y. Zhang, X. H. Tan, C. X. Huang, Y. Y. Xu and J. H. Shang, Apelin and apelin receptor in follicular granulosa cells of buffalo ovaries: Expression and regulation of steroidogenesis, *Front. Endocrinol.*, 2022, 13, 844360.
- 3 O. Wu, X. Lu, J. Leng, X. Zhang, W. Liu, F. Yang, H. Zhang, J. Li, S. Khederzadeh, X. Liu and C. Yuan, Reevaluating Adiponectin's impact on obesity hypertension: a

- Chinese case-control study, *BMC Cardiovasc. Disord.*, 2024, 24, 1–15.
- 4 U. F. Shaik Mohamed Sayed, S. Moshawih, H. P. Goh, N. Kifli, G. Gupta, S. K. Singh, D. K. Chellappan, K. Dua, A. Hermansyah, H. L. Ser, L. C. Ming and B. H. Goh, Natural products as novel anti-obesity agents: insights into mechanisms of action and potential for therapeutic management, *Front. Pharmacol.*, 2023, 14, 1182937.
- 5 R. M. Sete da Cruz, H. Ferreira, J. M. Jaski, M. C. E. Vieira, M. M. Pinc, S. G. H. de Souza and O. Alberton, Growth and phytochemistry of *Cymbopogon citratus* Stapf inoculated with plant growth-promoting bacteria under different lead levels, *Plants*, 2024, 13, 944.
- 6 O. S. Oladeji, F. E. Adelowo, D. T. Ayodele and K. A. Odelade, Phytochemistry and Pharmacology of Cymbopogon citratus: A review, Sci. Afr., 2019, 6, e00137.
- 7 G. Shah, R. Shri, V. Panchal, N. Sharma, B. Singh and A. S. Mann, Scientific basis for the therapeutic use of *Cymbopogon citratus*, Stapf (Lemon grass) *J. Adv. Pharm. Technol. Res.*, 2011, 2, 3–8.
- 8 Y. F. Madi, M. A. Choucry, S. A. El-Marasy, M. R. Meselhy and E. S. A. El-Kashoury, UPLC-Orbitrap HRMS metabolic profiling of *Cymbopogon citratus* cultivated in Egypt; neuroprotective effect against AlCl<sub>3</sub>-induced neurotoxicity in rats *J. Ethnopharmacol.*, 2020, 259, 112930.
- 9 G. Costa, J. P. Ferreira, C. Vitorino, M. E. Pina, J. J. Sousa, I. V. Figueiredo and M. T. Batista, Polyphenols from *Cymbopogon citratus* leaves as topical anti-inflammatory agents, *J. Ethnopharmacol.*, 2016, 178, 222–228.
- 10 M. W. Mashitah, N. Widodo, N. Permatasari and A. Rudijanto, Anti-obesity activity of *Cymbopogon citratus* (lemongrass): A systematic review, *J. Pharm. Pharmacogn. Res.*, 2024, **12**, 1090–1110.
- 11 S. Da Ressurreição, S. Pedreiro, M. T. Batista and A. Figueirinha, Effect of phenolic compounds from *Cymbopogon citratus* (DC) Stapf. Leaves on micellar solubility of cholesterol, *Molecules*, 2022, 27, 7338.
- 12 A. A. Adeneye and E. O. Agbaje, Hypoglycemic and hypolipidemic effects of fresh leaf aqueous extract of *Cymbopogon citratus* Stapf. in rats, *J. Ethnopharmacol.*, 2007, **112**, 440– 444.
- 13 V. S. Kumar, M. N. Inamdar and G. L. Viswanatha, Protective effect of lemongrass oil against dexamethasone induced hyperlipidemia in rats: Possible role of decreased lecithin cholesterol acetyl transferase activity, *Asian Pac. J. Trop. Med.*, 2011, 4, 658–660.
- 14 F. Pereira, L. Bedda, M. A. Tammam, A. K. Alabdullah, R. Arafa and A. El-Demerdash, Investigating the antiviral therapeutic potentialities of marine polycyclic lamellarin pyrrole alkaloids as promising inhibitors for SARS-CoV-2 and Zika main proteases (Mpro), *J. Biomol. Struct. Dyn.*, 2023, 42(8), 3983–4001.
- 15 M. A. Tammam, F. Pereira, O. Aly, M. Sebak, Y. M. Diab, A. Mahdy and A. El-Demerdash, Investigating the hepatoprotective potentiality of marine-derived steroids as prom-

ising inhibitors of liver fibrosis, *RSC Adv.*, 2023, **13**, 27477–27490.

- 16 Y. M. Diab, M. A. Tammam, A. M. Emam, M. A. Mohamed, M. E. Mahmoud, W. M. Semida, O. Aly and A. El-Demerdash, *Punica granatum L var nana*: A hepatoprotective and curative agent against CCl<sub>4</sub> induced hepatotoxicity in rats, *Egypt. J. Chem.*, 2022, 65, 723–733.
- 17 A. el Demerdash, A. M. Dawidar, E. M. Keshk and M. Abdel-Mogib, Gingerdione from the rhizomes of *Curcuma longa, Chem. Nat. Compd.*, 2012, **48**, 646–648.
- 18 A. El-Demerdash, C. Borde, G. Genta-Jouve, A. Escargueil and S. Prado, Cytotoxic constituents from the wheat plant pathogen *Parastagonospora nodorum* SN15, *Nat. Prod. Res.*, 2019, 36, 1273–1281.
- 19 A. El-Demerdash, G. Genta-Jouve, M. Bärenstrauch, C. Kunz, E. Baudouin and S. Prado, Highly oxygenated isoprenylated cyclohexanoids from the fungus *Parastagonospora nodorum* SN15, *Phytochemistry*, 2019, 166, 112056.
- 20 C. Moriou, D. Lacroix, S. Petek, A. El-Demerdash, R. Trepos, T. M. Leu, C. Florean, M. Diederich, C. Hellio, C. Debitus and A. Al-Mourabit, Bioactive bromotyrosine derivatives from the Pacific marine sponge *Suberea clavata* (Pulitzer-Finali, 1982), *Mar. Drugs*, 2021, 19, 143.
- 21 P. G. Reeves, Components of the AIN-93 diets as improvements in the AIN-76A diet, *J. Nutr.*, 1997, 127(5 Suppl), 838S-841S.
- 22 S. A. Zaitone and S. Essawy, Addition of a low dose of rimonabant to orlistat therapy decreases weight gain and reduces adiposity in dietary obese rats, *Clin. Exp. Pharmacol. Physiol.*, 2012, 39, 551–559.
- 23 H. Passing and W. Bablok, A new biometrical procedure for testing the equality of measurements from two different analytical methods. Application of linear regression procedures for method comparison studies in clinical chemistry, Part I, *J. Clin. Chem. Clin. Biochem.*, 1983, 21, 709– 720.
- 24 R. Yalow and W. Bauman, Diabetes Mellitus: Theory and Practice, Insulin in health and disease, in *Diabetes Mellitus: Theory and Practice*, ed. R. Yalow and W. A. Bauman, Excerpta Medica, New York, 1983.
- 25 D. R. Matthews, J. P. Hosker, A. S. Rudenski, B. A. Naylor, D. F. Treacher and R. C. Turner, Homeostasis model assessment: insulin resistance and  $\beta$ -cell function from fasting plasma glucose and insulin concentrations in man, Diabetologia, 1985, **28**, 412–419.
- 26 T. G. Cole, I. Kuisk, W. Patsch and G. Schonfeld, Effects of high cholesterol diets on rat plasma lipoproteins and lipoprotein-cell interactions, *J. Lipid Res.*, 1984, 25, 593–603.
- 27 W. T. Friedewald, R. I. Levy and D. S. Fredrickson, Estimation of the concentration of low-density lipoprotein cholesterol in plasma, without use of the preparative ultracentrifuge, *Clin. Chem.*, 1972, 18, 499–502.
- 28 K.-O. Kim, Y.-A. Kim and H. Lee, Isoflavone-rich bean sprout cookie improves lipid metabolism in hyperlipidemic rat, *FASEB J.*, 2007, **21**, A1087–A1087.

- 29 M. F. Lopes-Virella, P. Stone, S. Ellis and J. A. Colwell, Cholesterol determination in high-density lipoproteins separated by three different methods, *Clin. Chem.*, 1977, 23, 882–884.
- 30 N. Mellouk, C. Rame, J. L. Touzé, E. Briant, L. Ma, D. Guillaume, D. Lomet, A. Caraty, T. Ntallaris, P. Humblot and J. Dupont, Involvement of plasma adipokines in metabolic and reproductive parameters in Holstein dairy cows fed with diets with differing energy levels, *J. Dairy Sci.*, 2017, 100, 8518–8533.
- 31 R. Levesque, SPSS programming and data management: A guide for SPSS and SAS users, in *Ibm Spss*, 2005, pp. 1–520.
- 32 G. Paget and R. Thomson, Standard operating procedures in pathology: including developmental toxicology and quality assurance.1979.
- 33 R. H. Mekky, E. Abdel-Sattar, A. Segura-Carretero and M. D. M. Contreras, Metabolic profiling of the oil of sesame of the Egyptian cultivar 'Giza 32' employing LC-MS and tandem MS-Based untargeted method, *Foods*, 2021, 10, 298.
- 34 R. H. Mekky, E. Abdel-Sattar, A. Segura-Carretero and M. Del Mar Contreras, Phenolic compounds from sesame cake and antioxidant activity: A new insight for agri-food residues' significance for sustainable development, *Foods*, 2019, **8**, 432.
- 35 R. H. Mekky, M. D. M. Contreras, M. R. El-Gindi, A. R. Abdel-Monem, E. Abdel-Sattar and A. Segura-Carretero, Profiling of phenolic and other compounds from Egyptian cultivars of chickpea (*Cicer arietinum* L.) and antioxidant activity: a comparative study, *RSC Adv.*, 2015, 5, 17751–17767.
- 36 R. H. Mekky, M. M. Thabet, C. Rodríguez-Pérez, D. M. Y. Elnaggar, E. A. Mahrous, A. Segura-Carretero and E. Abdel-Sattar, Comparative metabolite profiling and antioxidant potentials of seeds and sprouts of three Egyptian cultivars of *Vicia faba* L, *Food Res. Int.*, 2020, 136, 109537.
- 37 J. Eberhardt, D. Santos-Martins, A. F. Tillack and S. Forli, AutoDock Vina 1.2.0: New docking methods, expanded force field, and python bindings, *J. Chem. Inf. Model.*, 2021, 61, 3891–3898.
- 38 RDKit: Open-Source Cheminformatics Software | BibSonomy, https://www.bibsonomy.org/bibtex/ 28d01fceeccd6bf2486e47d7c4207b108/salotz, (accessed 14 September 2024).
- 39 E. C. Meng, T. D. Goddard, E. F. Pettersen, G. S. Couch, Z. J. Pearson, J. H. Morris and T. E. Ferrin, UCSF ChimeraX: Tools for structure building and analysis, *Protein Sci.*, 2023, 32, e4792.
- 40 M. F. Adasme, K. L. Linnemann, S. N. Bolz, F. Kaiser, S. Salentin, V. J. Haupt and M. Schroeder, PLIP 2021: expanding the scope of the protein-ligand interaction profiler to DNA and RNA, *Nucleic Acids Res.*, 2021, 49, W530– W534.
- 41 Y. Myung, A. G. C. de Sá and D. B. Ascher, Deep-PK: deep learning for small molecule pharmacokinetic and toxicity prediction, *Nucleic Acids Res.*, 2024, **2024**, 1–7.

42 N. R. Kohan, S. Nazifi, M. R. Tabandeh and M. A. Lari, Effect of L-carnitine supplementation on apelin and apelin receptor (Apj) expression in cardiac muscle of obese diabetic rats, Cell J., 2018, 20, 427–434.

**Food & Function** 

- 43 M. P. Czech, Insulin action and resistance in obesity and type 2 diabetes, *Nat. Med.*, 2017, 23, 804–814.
- 44 R. Naz, F. Saqib, S. Awadallah, M. Wahid, M. F. Latif, I. Iqbal and M. S. Mubarak, Food polyphenols and type ii diabetes mellitus: Pharmacology and mechanisms, *Molecules*, 2023, **28**, 3996.
- 45 A. A. Adeneye and E. O. Agbaje, Hypoglycemic and hypolipidemic effects of fresh leaf aqueous extract of *Cymbopogon citratus* Stapf. in rats, *J. Ethnopharmacol.*, 2007, **112**, 440–444.
- 46 C. Ewenighi, U. Dimkpa, J. Onyeanusi, L. Onoh, G. Onoh and U. Ezeugwu, Estimation of glucose level and body weight in alloxan induced diabetic rat treated with aqueous extract of *Garcinia kola* Seed, *Ulutas Med. J.*, 2015, 1, 26.
- 47 M. Machraoui, Z. Kthiri, M. Ben Jabeur and W. Hamada, Ethnobotanical and phytopharmacological notes on *Cymbopogon citratus* (DC.) Stapf, *J. New Sci.*, 2018, 55, 3642–3652.
- 48 B. Middleton and H. Kok-Pheng, Evidence for binding of certain acidic drugs to α1-acid glycoprotein, *Biochem. Pharmacol.*, 1982, 31, 2897–2901.
- 49 C. E. Elson, G. L. Underbakke, P. Hanson, E. Shrago, R. H. Wainberg and A. A. Qureshi, Impact of lemongrass oil, an essential oil, on serum cholesterol *Lipids*, 1989, 24, 677–679.
- 50 R. P. Pereira, R. Fachinetto, A. De Souza Prestes, R. L. Puntel, G. N. Santos Da Silva, B. M. Heinzmann, T. K. Boschetti, M. L. Athayde, M. E. Bürger, A. F. Morel, V. M. Morsch and J. B. T. Rocha, Antioxidant effects of different extracts from *Melissa officinalis*, *Matricaria recutita* and *Cymbopogon citratus*, *Neurochem. Res.*, 2009, 34, 973– 983.
- 51 N. Ranjbar Kohan, M. R. Tabandeh, S. Nazifi and Z. Soleimani, L-carnitine improves metabolic disorders and regulates apelin and apelin receptor genes expression in adipose tissue in diabetic rats, *Physiol. Rep.*, 2020, 8, e14641.
- 52 K. Mehri, G. Hamidian, Z. Zavvari Oskuye, S. Nayebirad and F. Farajdokht, The role of apelinergic system in metabolism and reproductive system in normal and pathological conditions: an overview, *Front. Endocrinol.*, 2023, 14, 1193150.
- 53 P. C. Arica, S. Aydin, U. Zengin, A. Kocael, A. Orhan, K. Zengin, R. Gelisgen, M. Taskin and H. Uzun, The effects on obesity related peptides of laparoscopic gastric band applications in morbidly obese patients, *J. Invest. Surg.*, 2018, 31, 89–95.
- 54 J. Boucher, B. Masri, D. Daviaud, S. Gesta, C. Guigné, A. Mazzucotelli, I. Castan-Laurell, I. Tack, B. Knibiehler, C. Carpéné, Y. Audigier, J. S. Saulnier-Blache and P. Valet, Apelin, a newly identified adipokine up-regulated by insulin and obesity, *Endocrinology*, 2005, 146, 1764–1771.

- 55 Z. Kochan and J. Karbowska, Dehydroepiandrosterone upregulates resistin gene expression in white adipose tissue, *Mol. Cell. Endocrinol.*, 2004, **218**, 57–64.
- 56 T. R. Kumar, J. Agno, J. A. Janovick, P. M. Conn and M. M. Matzuk, Regulation of FSHbeta and GnRH receptor gene expression in activin receptor II knockout male mice, *Mol. Cell. Endocrinol.*, 2003, 212, 19–27.
- 57 M. Matsuda, I. Shimomura, M. Sata, Y. Arita, M. Nishida, N. Maeda, M. Kumada, Y. Okamoto, H. Nagaretani, H. Nishizawa, K. Kishida, R. Komuro, N. Ouchi, S. Kihara, R. Nagai, T. Funahashi and Y. Matsuzawa, Role of adiponectin in preventing vascular stenosis. The missing link of adipovascular axis, *J. Biol. Chem.*, 2002, 277, 37487–37491.
- 58 N. Ouchi and K. Walsh, Adiponectin as an anti-inflammatory factor, *Clin. Chim. Acta*, 2007, **380**, 24–30.
- 59 Y. Yamamoto, H. Hirose, I. Saito, M. Tomita, M. Taniyama, K. Matsubara, Y. Okazaki, T. Ishii, K. Nishikai and T. Saruta, Correlation of the adipocyte-derived protein adiponectin with insulin resistance index and serum high-density lipoprotein-cholesterol, independent of body mass index, in the Japanese population, *Clin. Sci.*, 2002, 103, 137–142.
- 60 S. Lee and H.-B. Kwak, Role of adiponectin in metabolic and cardiovascular disease, *J. Exerc. Rehabil.*, 2014, **10**, 54.
- 61 C. K. Chakraborti, Role of adiponectin and some other factors linking type 2 diabetes mellitus and obesity, *World J. Diabetes*, 2015, **6**, 1296.
- 62 J. A. Falode, T. B. Olofinlade, G. S. Fayeun, A. O. Adeoye, F. A. Bamisaye, O. R. Ajuwon and T. O. Obafemi, Free and bound phenols from *Cymbopogon citratus* mitigated hepatocellular injury in streptozotocin-induced type 1 diabetic male rats via decrease in oxidative stress, inflammation, and other risk markers, *Pharmacol. Res. Mod. Chin. Med.*, 2023, 7, 100234.
- 63 B. Y. Sheikh, The role of prophetic medicine in the management of diabetes mellitus: A review of literature, *J. Taibah Univ. Med. Sci.*, 2016, 11, 339–352.
- 64 S. Hussain, W. Javed, A. Tajammal, M. Khalid, N. Rasool, M. Riaz, M. Shahid, I. Ahmad, R. Muhammad and S. A. A. Shah, Synergistic antibacterial screening of *Cymbopogon citratus* and *Azadirachta indica*: Phytochemical profiling and antioxidant and hemolytic activities, *ACS Omega*, 2023, 8, 16600–16611.
- 65 A. Tej, R. H. Mekky, M. del M. Contreras, A. Feriani, M. Tir, B. L'taief, M. O. Alshaharni, B. Faidi, K. Mnafgui, Z. Abbes, E. Saadaoui, M. A. Borgi and N. Tlili, *Eucalyptus torquata* seeds: Investigation of phytochemicals profile via LC-MS and its potential cardiopreventive capacity in rats, *Food Biosci.*, 2024, 59, 103666.
- 66 R. Hassan Mekky, E. Abdel-Sattar, A. Segura-Carretero and M. del M. Contreras, A comparative study on the metabolites profiling of linseed cakes from Egyptian cultivars and antioxidant activity applying mass spectrometry-based analysis and chemometrics, *Food Chem.*, 2022, 395, 133524.
- 67 Reaxys, https://www.reaxys.com/#/search/quick, (accessed 19 April 2024).

- 68 KNApSAcK Core System, https://www.knapsackfamily.com/knapsack\_core/top.php, (accessed 19 April 2024).
- 69 P. Okińczyc, J. Widelski, M. Ciochoń, E. Paluch, A. Bozhadze, M. Jokhadze, G. Mtvarelishvili, I. Korona-Głowniak, B. Krzyżanowska and P. M. Kuś, Phytochemical profile, plant precursors and some properties of Georgian propolis, *Molecules*, 2022, 27, 7714.
- 70 F. Cuyckens and M. Claeys, Mass spectrometry in the structural analysis of flavonoids, *J. Mass Spectrom.*, 2004, **39**, 1–15.
- 71 N. M. Fayek, R. H. Mekky, C. N. Dias, M. Kropf, A. G. Heiss, L. A. Wessjohann and M. A. Farag, UPLC-MS metabolomebased seed classification of 16 *Vicia* Species: A prospect for phyto-equivalency and chemotaxonomy of different accessions, *J. Agric. Food Chem.*, 2021, 69, 5252–5266.